Extragalactic surveys with CMB experiments

Gianfranco De Zotti
National Astrophysics Institute (INAF)
Padua Astronomical Observatory

Thanks to Matteo Bonato and Mattia Negrello

Extragalactic surveys with CMB missions

- **Broad spectral range hardly, if at all, accessible from the ground and only lightly covered by other space missions.**
- **All-sky coverage, ideal to look for rare phenomena.**
- **Poor (but not too much) angular resolution that can be both a limitation and a resource.**
- **Angular resolution is the key for extragalactic surveys.**

Extragalactic surveys with CMB missions - 2

- **Two main populations of extragalactic sources: radio sources (mostly blazars), dominating up to about 150- 200 GHz, and active star-forming galaxies dominating at higher frequencies**
- **Planck has already provided unique information on these source populations**

Extragalactic source populations

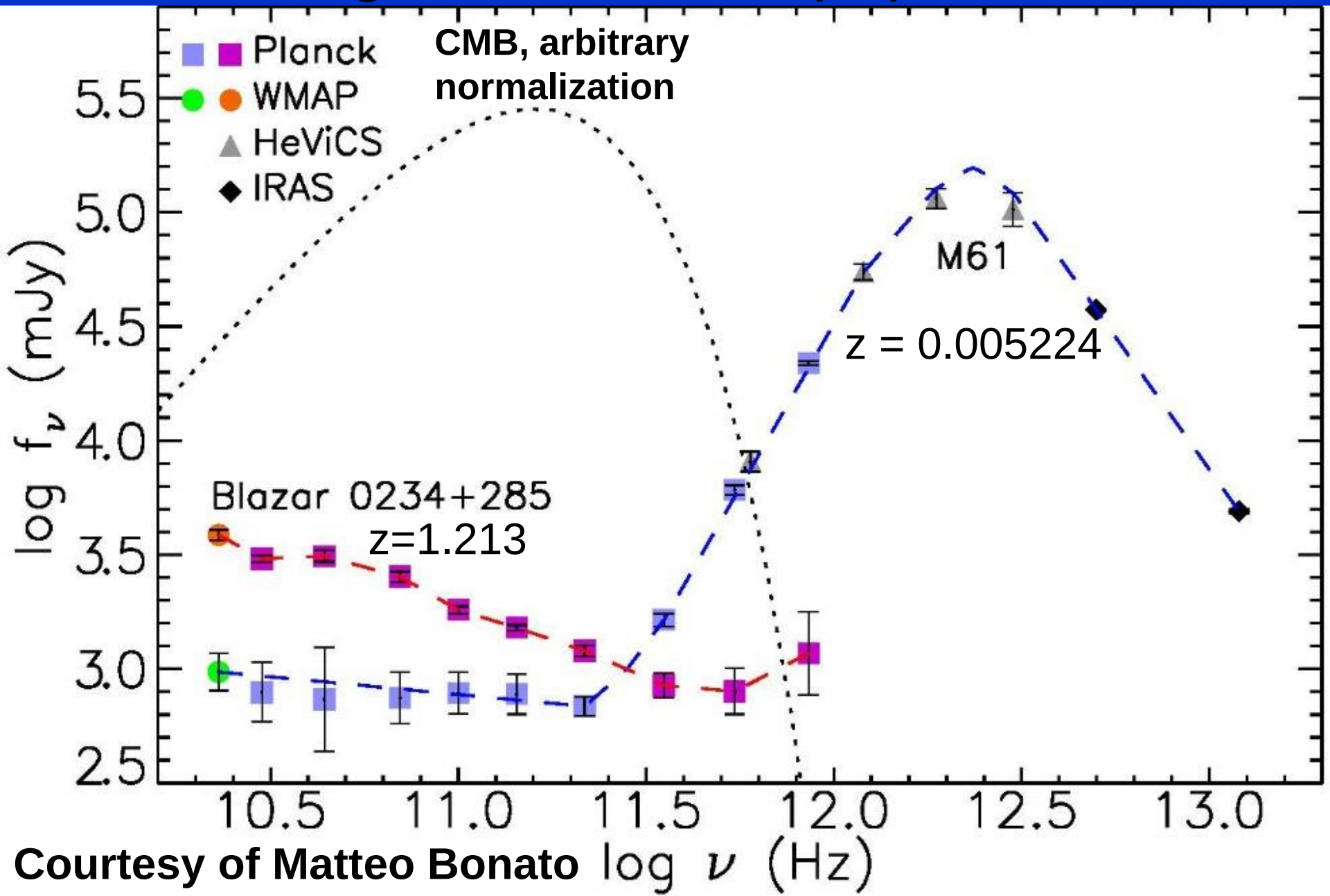

Courtesy of Matteo Bonato

Source counts

Dusty galaxies

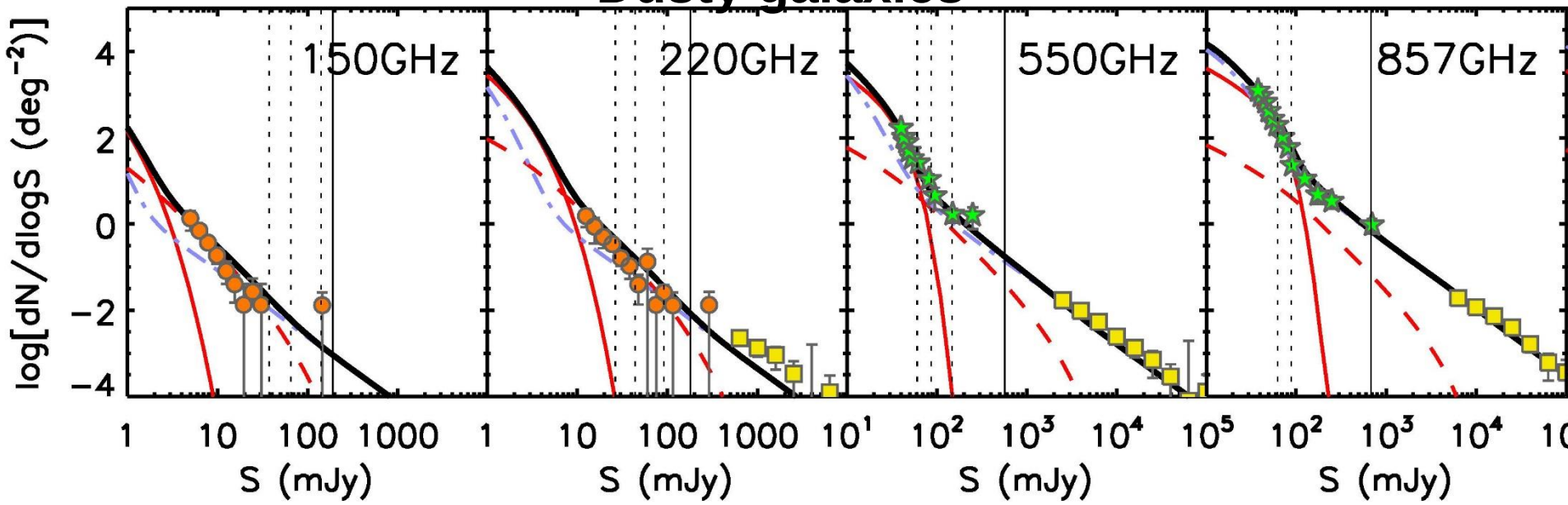

Radio sources

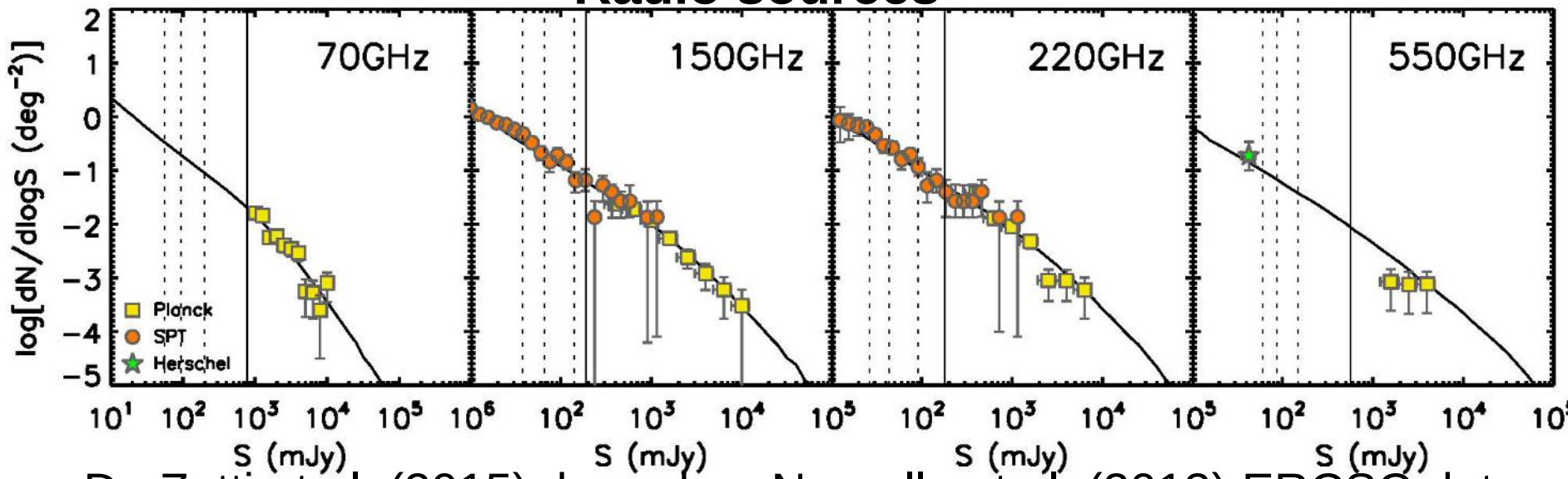

De Zotti et al. (2015), based on Negrello et al. (2013) ERCSC data

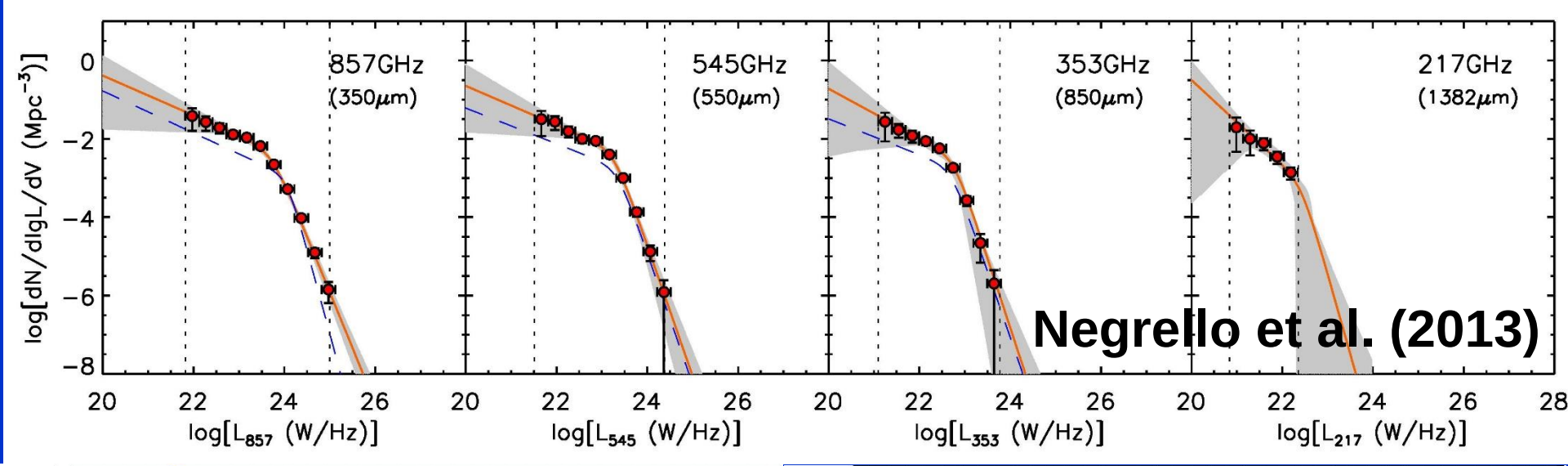

Negrello et al. (2013)

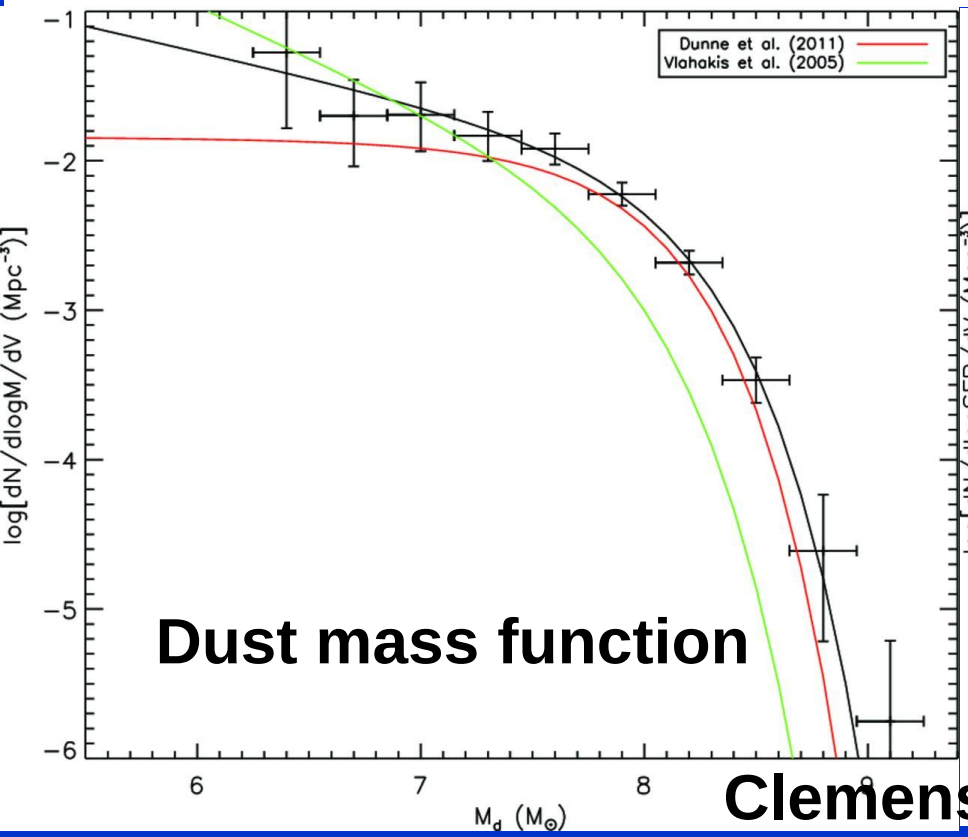

Dust mass function

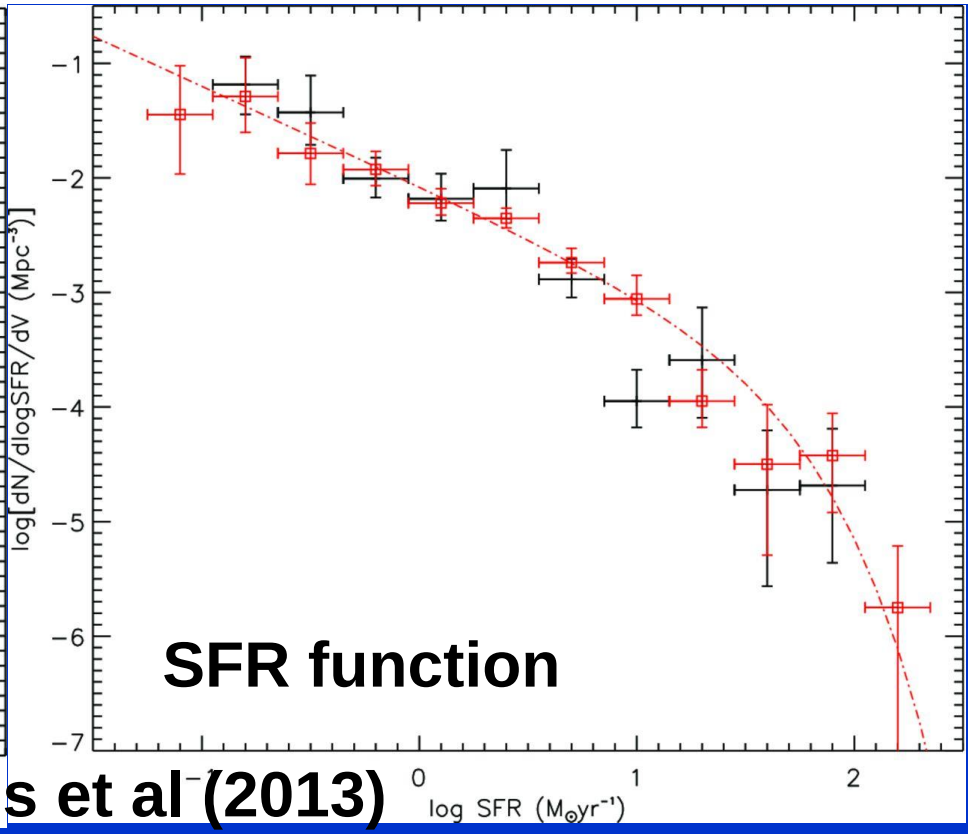

SFR function

Clemens et al (2013)

Source counts

Strongly lensed galaxies

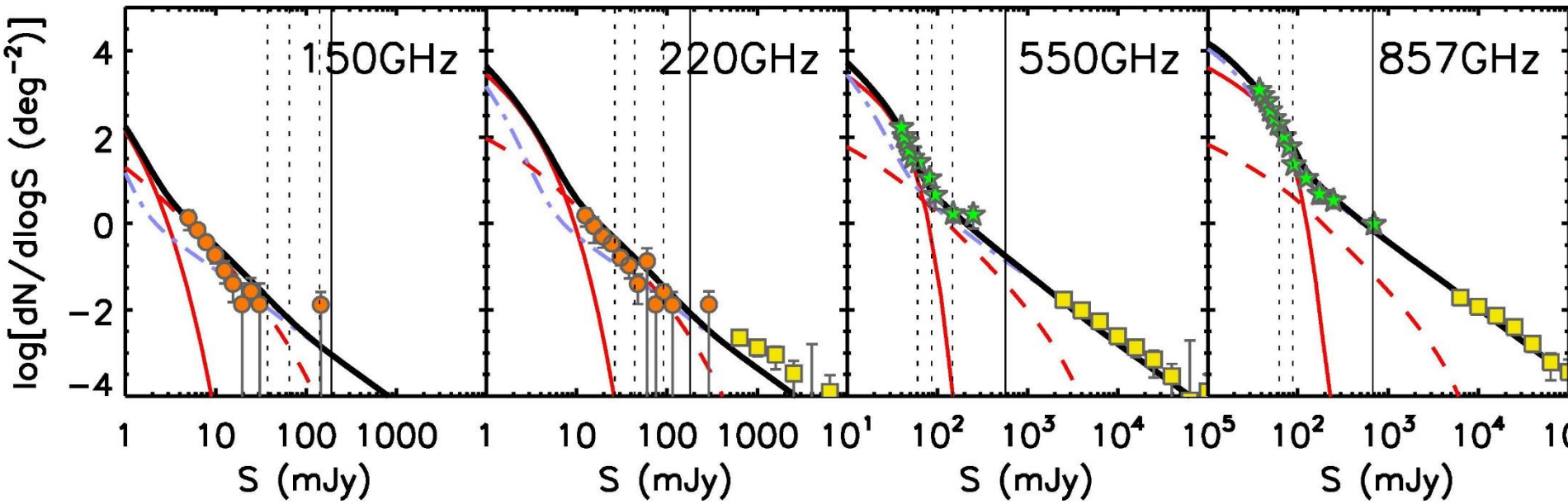

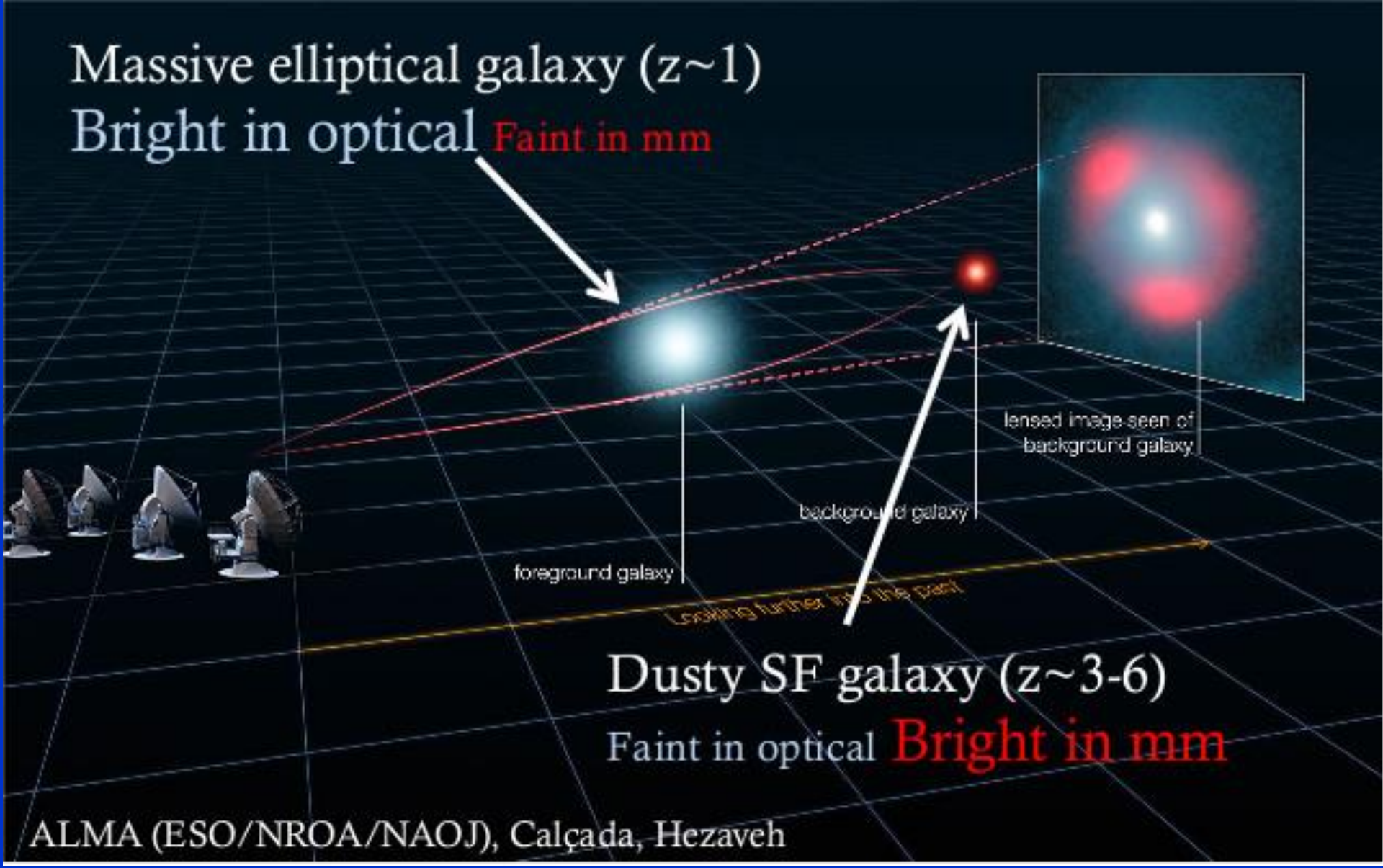

Background sources are essentially invisible in the optical while lenses are essentially invisible in the far-IR/sub-mm.

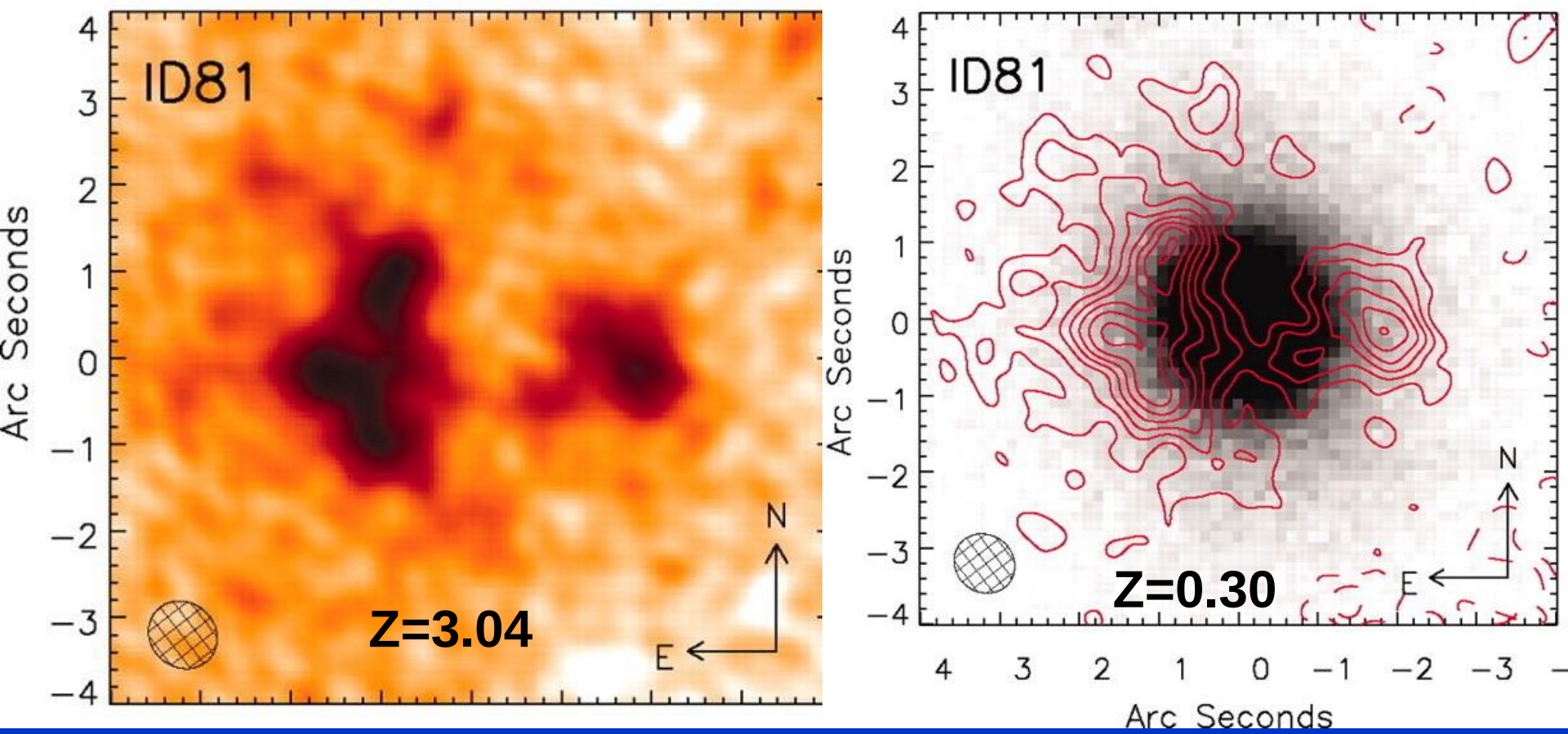

Sub-mm (SMA, left panel) and optical imaging of the strongly-lensed galaxy ID81 detected by the *Herschel-ATLAS* survey. The Keck i-band image is shown in the right-hand panel with the SMA contours superimposed (in red). The contours are in steps of 2σ. The SMA beam is shown in the bottom-left corner. From Negrello et al. (2010, 2014).

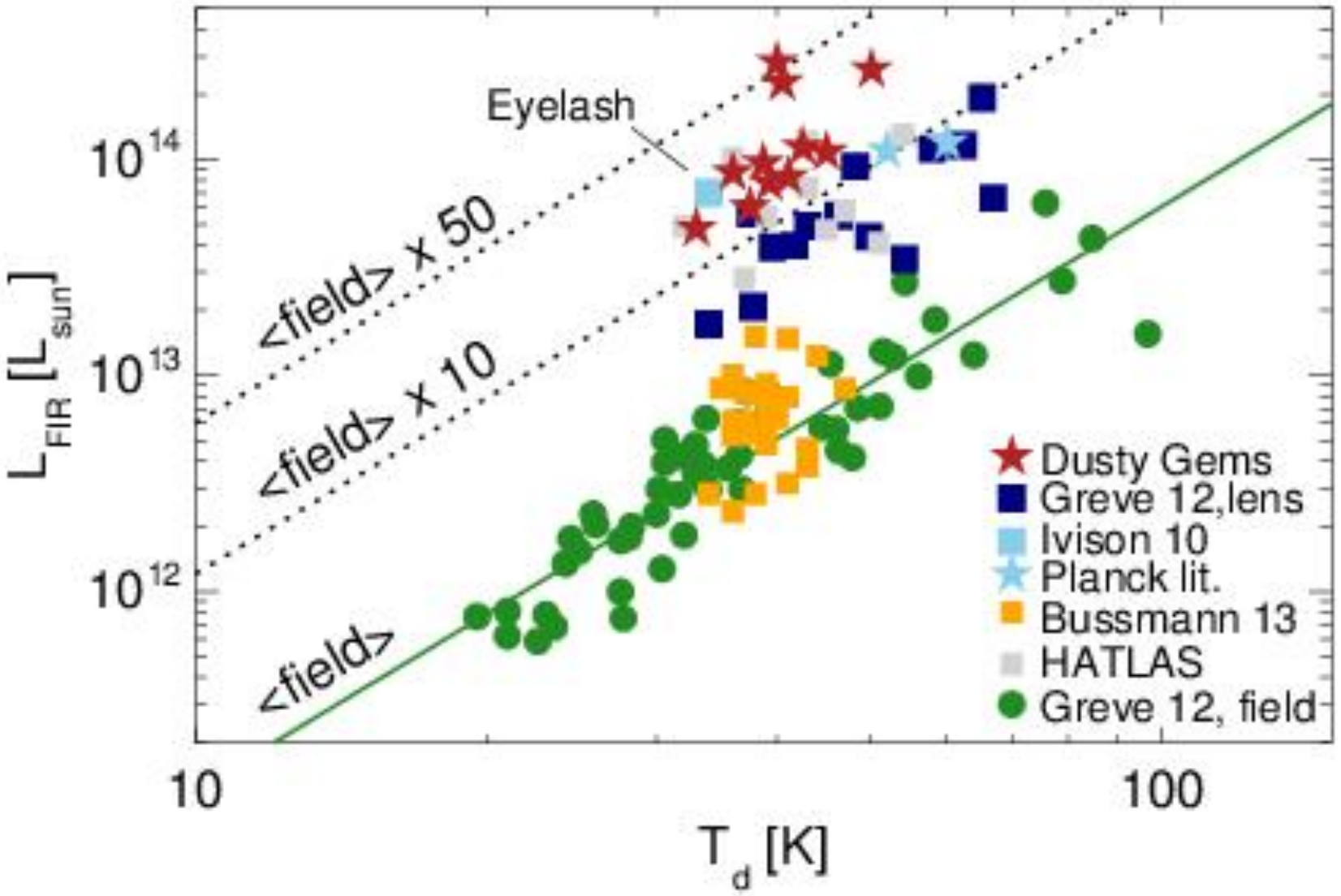

Dusty Gems: 11 strongly gravitationally lensed galaxies at z= 2.2 – 3.6 detected by Planck (Cañameras et al. 2015)

The virtues of gravitational lensing - 1

Planck has demonstrated the existence of extreme, strongly-lensed, high-z galaxies, with estimated gravitational amplifications, μ, of up to 50.

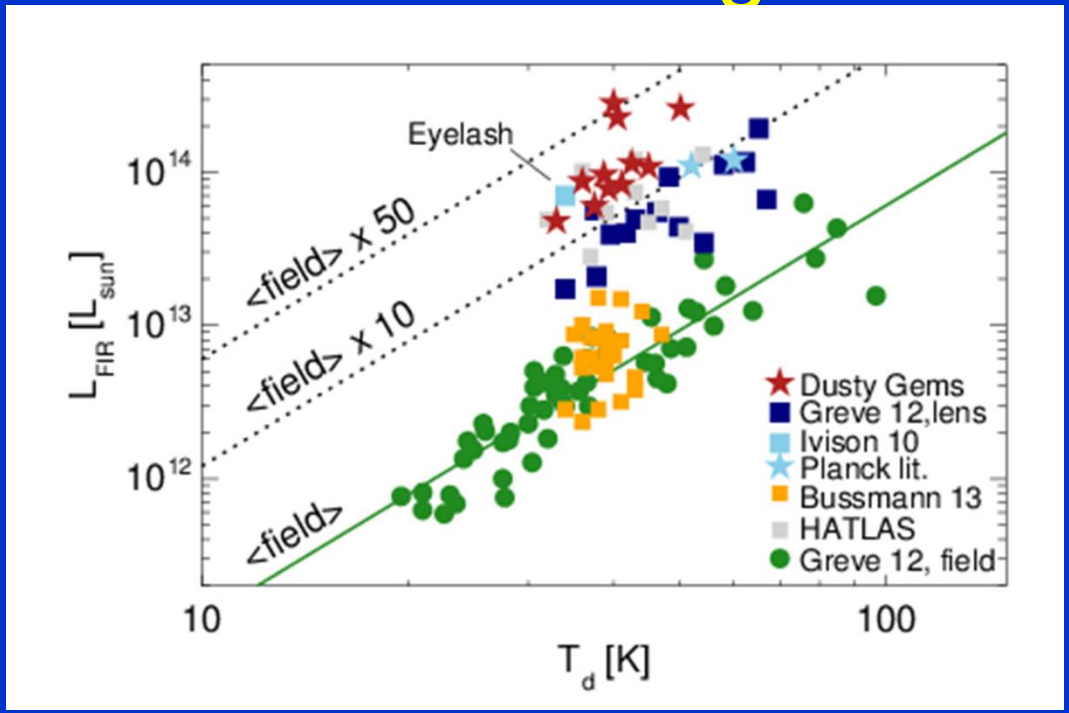

Surveys over limited areas miss these very rare objects. Strong lensing offers the opportunity of detailed follow-up studies of high-z galaxies with otherwise unattainable sensitivity: the exposure time to reach a given flux density limit varies as μ^{-2} and, since lensing conserves surface brightness, it stretches the image, thus effectively increasing the angular resolution by a factor $\mu^{1/2}$ (actually the amplification is mostly in one dimension).

The virtues of gravitational lensing - 2

Strong lensing is a powerful tool to address major astrophysical issues (cf. Treu 2010):

- studying distant galaxies, black holes, and active nuclei that are too small or too faint to be resolved or detected with current instrumentation;
- strong lensing observables (relative positions, flux ratios, time delays between multiple images) depend on the gravitational potential of the foreground galaxy (lens) and its derivatives; thus strong lensing allows us to understand the spatial distribution of mass at kpc and sub-kpc scale, where baryons and dark matter interact to shape galaxies as we see them;
- the lensing observables also depend on the overall geometry of the Universe via angular diameter distances between observer, lens and source; thus we can derive information on the overall geometry, content, and kinematics of the Universe.

How to do better than Planck?

- With current instrumentation sensitivity is not an issue: already for Planck the detection limit was set not by sensitivity but by ″confusion″ (fluctuations due to sources below the detection limit and to other components).

- At frequencies and angular scales of interest the ″confusion″ scales roughly as the FWHM^2. For diffraction-limited observations FWHM $\propto\lambda$/D, D being the size of the telescope.

- Planck was diffraction-limited only up to 217 GHz. For example, at 545 and 857 GHz (550 and 350 μm), where dusty galaxies are brightest and easiest to detect, the Planck beam has an effective FWHM of 4.83′ and 4.64′, while the diffraction limits for its 1.5-m telescope are of 1.5′ and 1.0′, respectively.

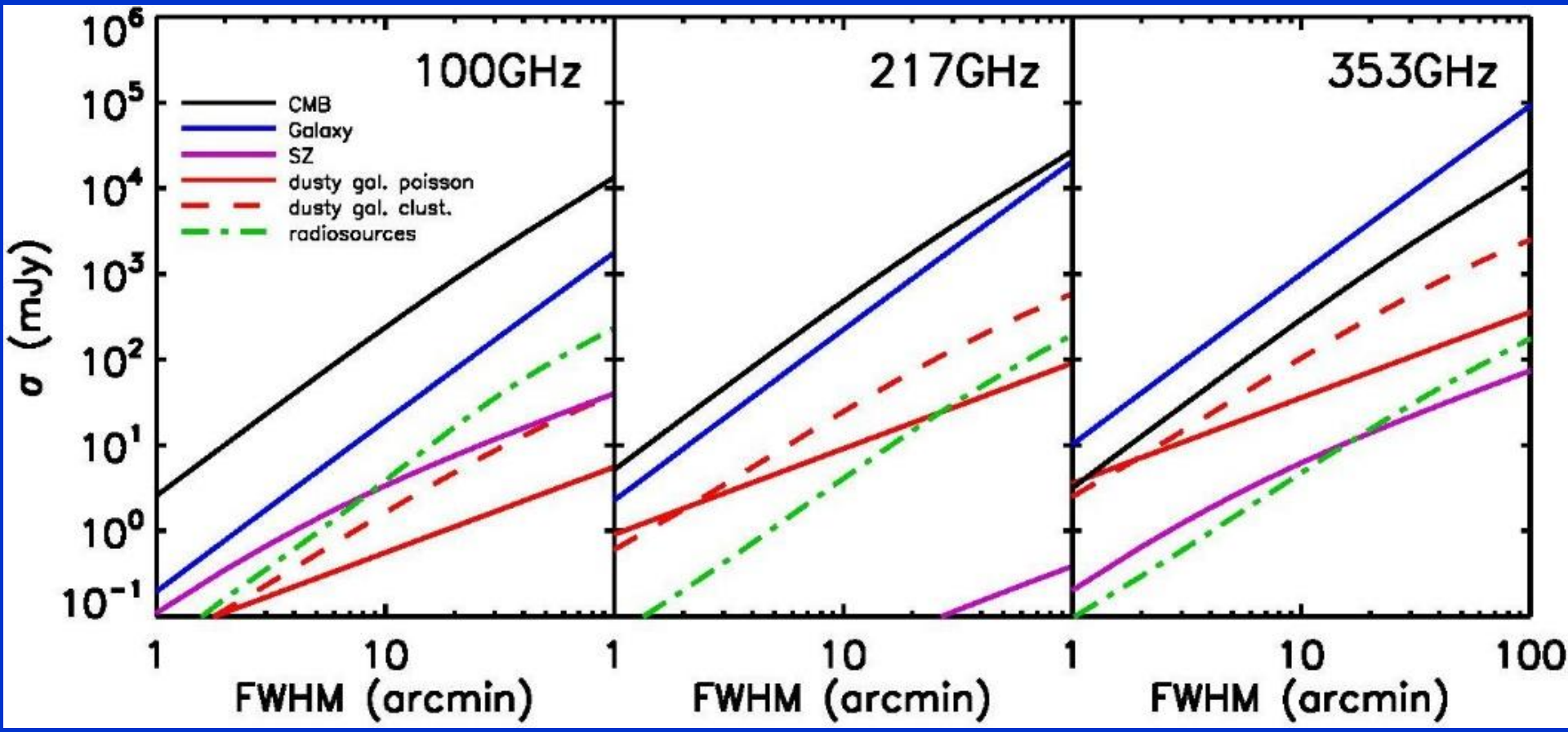

De Zotti et al. (2016)

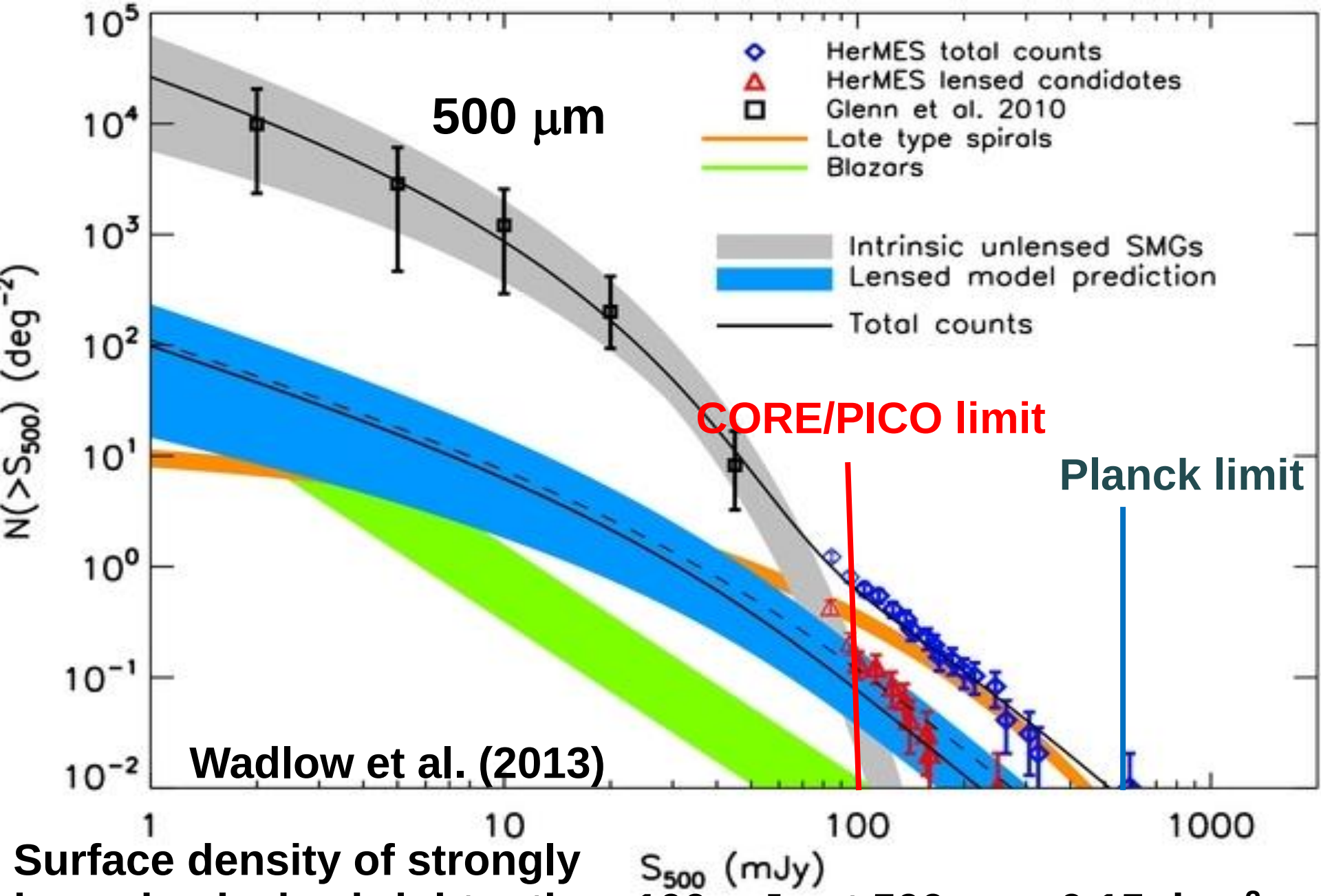

Surface density of strongly lensed galaxies brighter than 100 mJy at 500μm ≈0.15 deg^{-2}

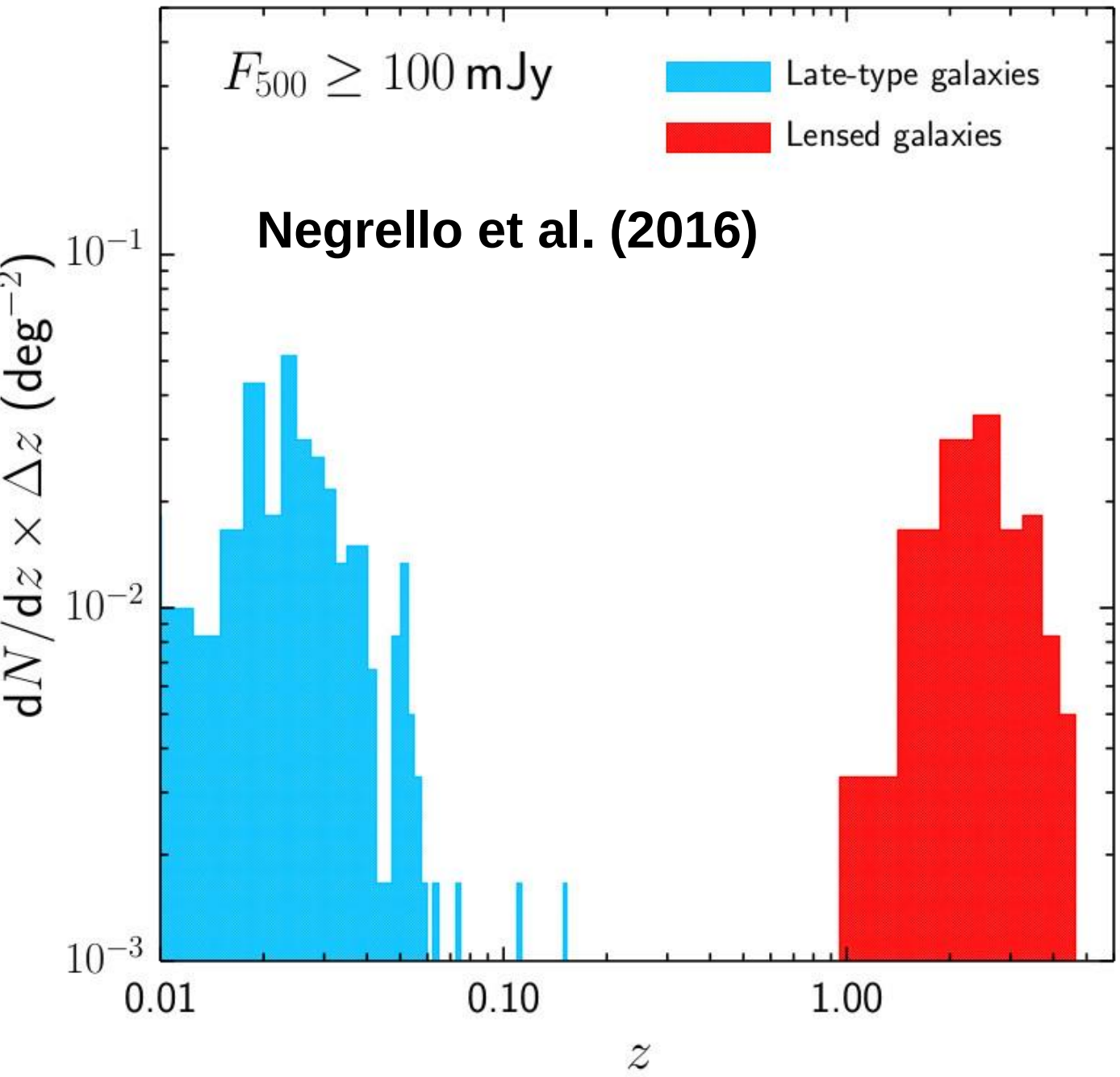

Separation of strongly lensed from local galaxies very easy: local alaxies immediately recognized in shallow optical images.

Proto-clusters of galaxies

Proto-clusters

- No unique definition. We call proto-clusters structures evolving towards the present day configuration of rich galaxy clusters, i.e. massive over-densities of star forming galaxies. not necessarily virialized (but will virialize at some stage).

- Low angular resolution sub-mm surveys are best for such objects: at higher resolution a substantial fraction of the cluster luminosity. The sub-mm flux densities of proto-cluster candidates measured by Planck are about 2 to 3 times larger than the summed luminosities of member galaxies detected with Herschel within the Planck beam (Clements et al. 2014, Planck Coll. XXXIX 2015) .

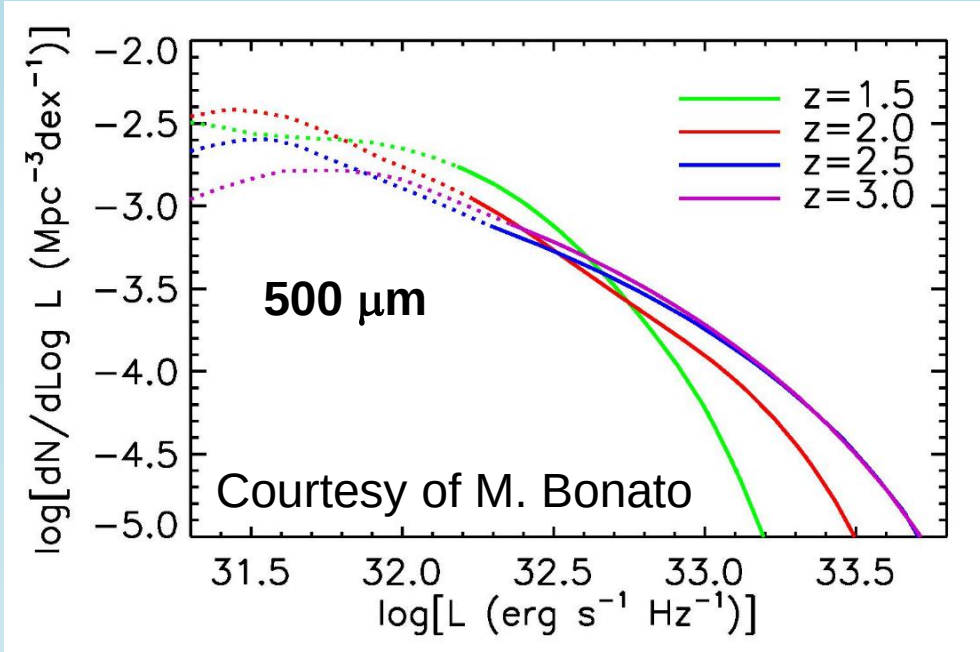

Portions of the galaxy LF at various z covered by Herschel surveys to a flux limit of 50 mJy at 500 μm. The corresponding luminosity density is 29, 43, 66 and 67%, from z=1.5 to z=3, respectively, of the total luminosity density. Figure courtesy of Matteo Bonato.

- High-z massive proto-clusters are rare ⇒ need of very large area surveys ⇒ the role of Planck.

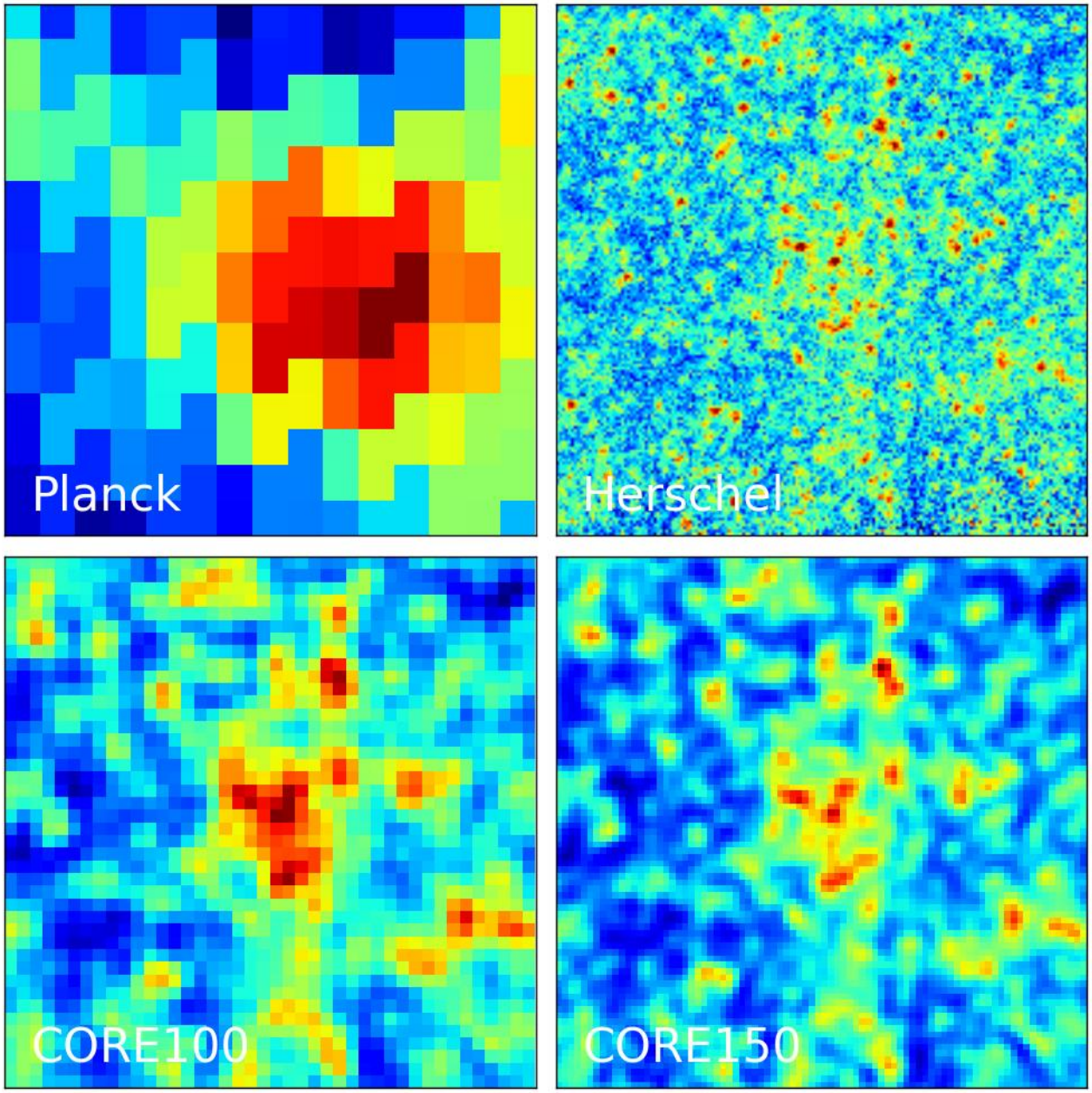

Planck (upper left panel) and Herschel (upper right panel) images at 857 and 600 GHz, respectively, of a candidate z = 2.3 proto-cluster in the Bootes field of the HerMES survey Clements et al. (2014), compared with the appearance it may take at 600 GHz for the diffraction limited beams of CORE with a 100 cm and a 150 cm effective diameter of the telescope. The size of each map is 25′× 25′. Figure from De Zotti et al. (2016).

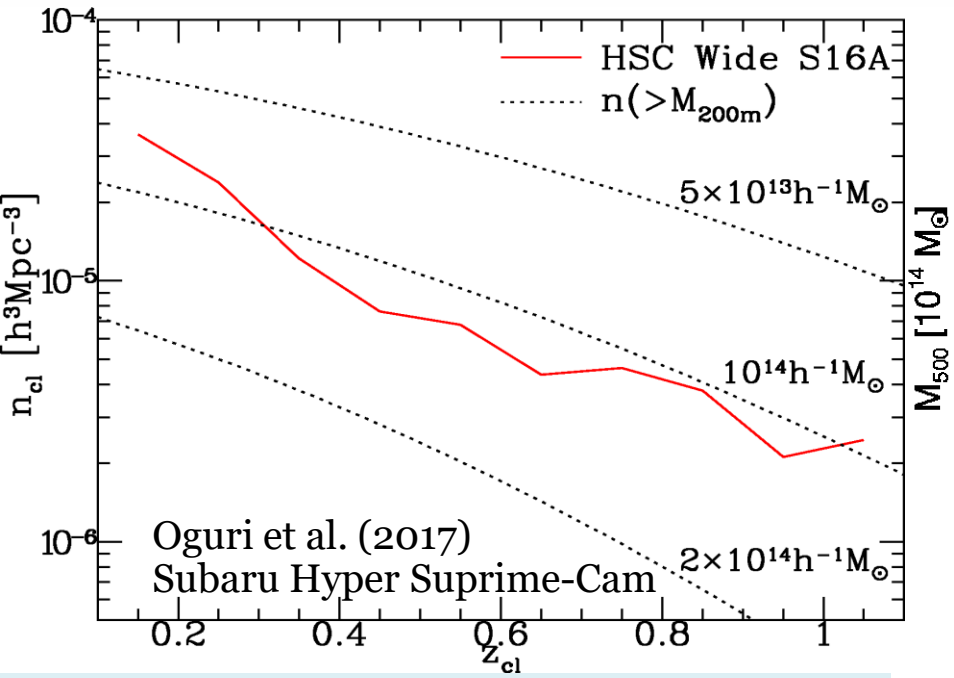

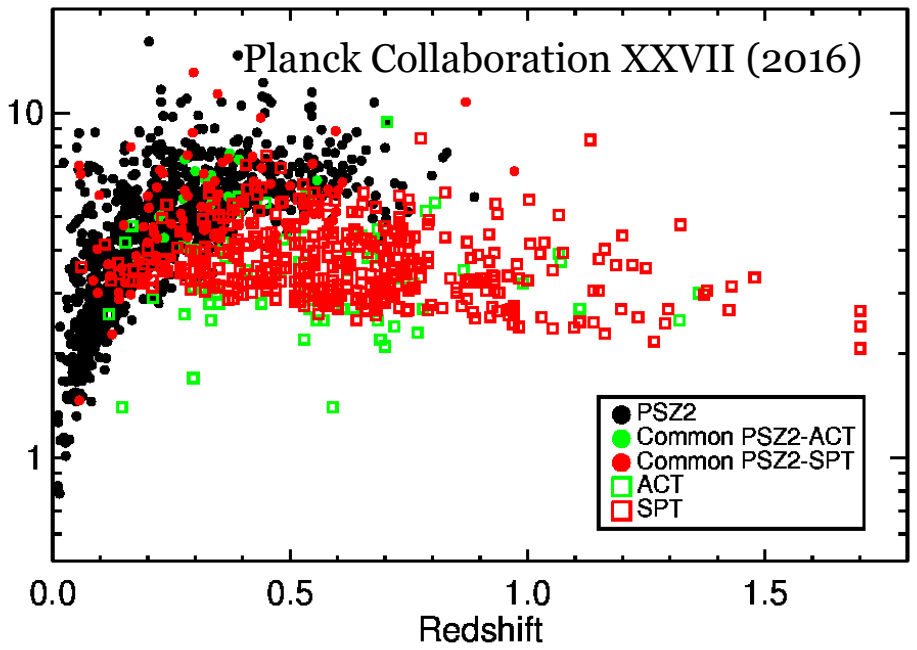

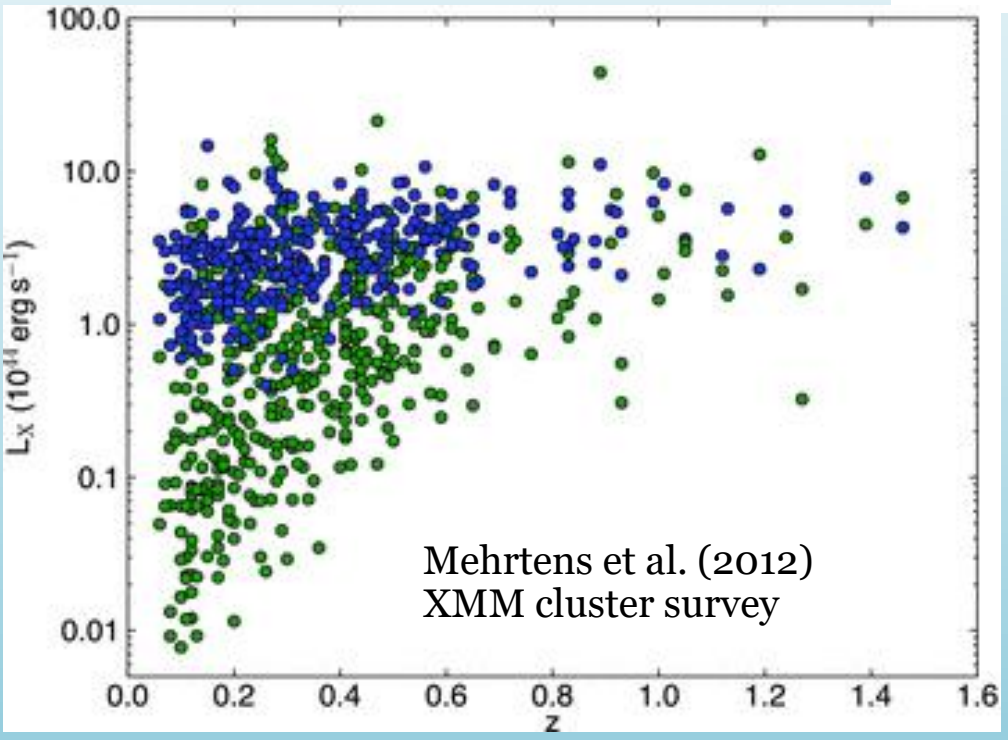

Classical techniques for detecting galaxy clusters (optical/near-IR "red sequence", X-ray emission, SZ effect) preferentially or exclusively select evolved objects, with mature galaxy populations and a hot intra-cluster medium. As a result, most known clusters are at redshifts <1.5, i.e. below that of the peak of global star-formation activity.

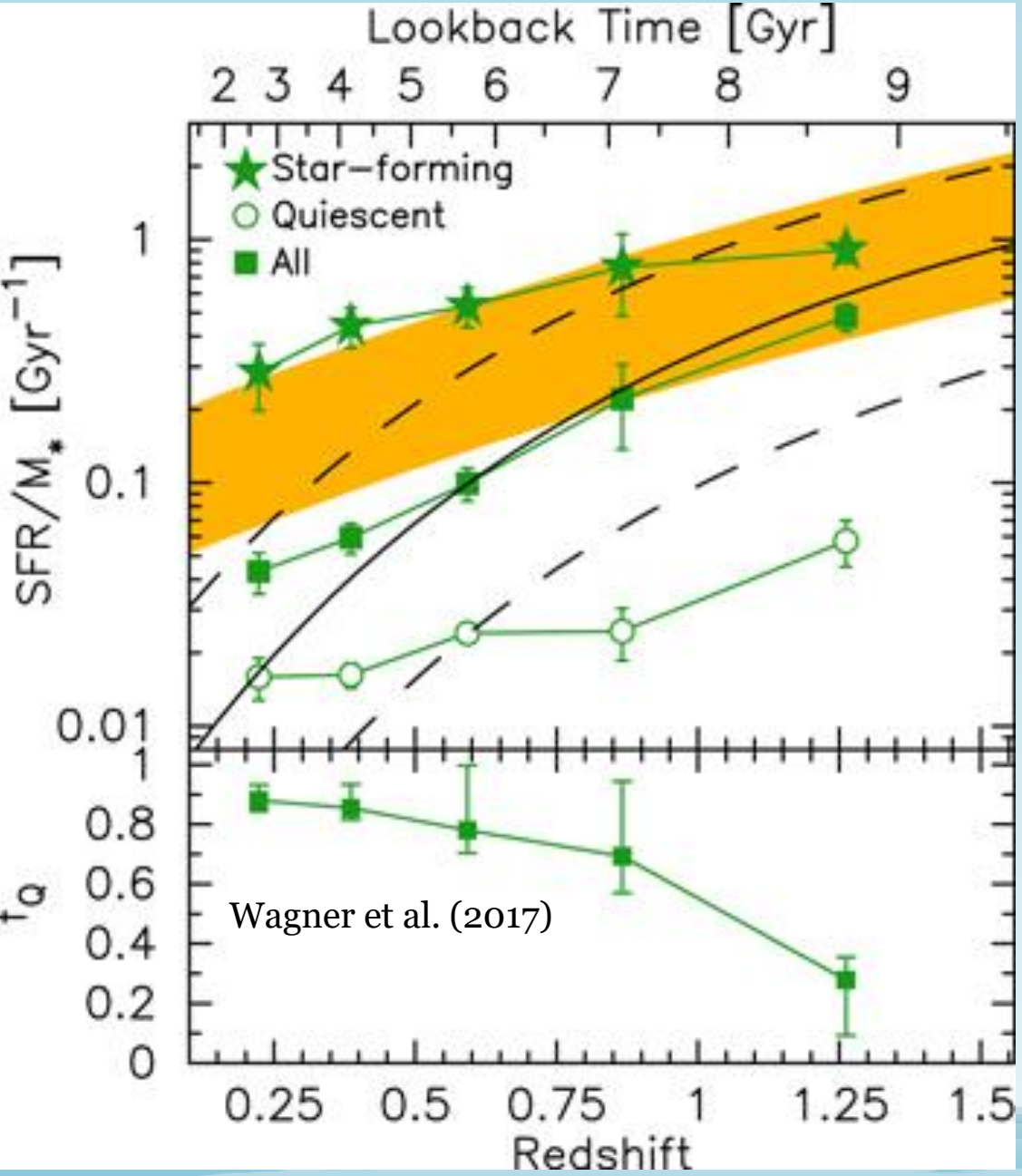

Upper panel: specific SFR vs. redshift for different cluster galaxies and the overall cluster population. The gold shaded region shows the SF main sequence from Elbaz et al. (2011). The overall cluster specific SFR (sSFR) is in excellent agreement with the Alberts et al. (2014) fit of sSFR vs. redshift for cluster galaxies (solid black curve; dashed curves are 1σ uncertainty).

Lower panel: fraction of quiescent cluster galaxies vs. redshift. The quiescent population builds up quickly at earlier times, with fractions gradually increasing to more recent times.

The mean sSFR of cluster galaxies evolves substantially faster that that in the field, due to the rapidly decreasing fraction of quiescent galaxies**.** For $z<1.2$, $SFR_{cluster}/SFR_{field} \propto (1+z)^{3.8}$, $SFR_{field} \propto (1+z)^3$, so that $\mathbf{SFR_{cluster} \propto (1+z)^{6.8}}$. At higher z (up to z ~1.75) the star formation in cluster galaxies is largely consistent with that of field galaxies at similar epochs, albeit with quite strong variations in star formation from cluster to cluster (Alberts et al. 2016).

This implies that:

- **The best way to detect high-z (proto-)clusters is to look for sub-mm intensity peaks without a local galaxy counterpart**. But the Planck experience shows that we need a resolution ~1′.
- Low resolution sub-mm surveys provide key information on the **evolution with z of star-formation of galaxies in dense environments**; at present such information is available only for small samples over limited redshift ranges.
- **Dust emission biases measurements of the tSZ effect** as already seen in Planck data, albeit at low level as expected since clusters are mostly at $z \leq 0.4$.

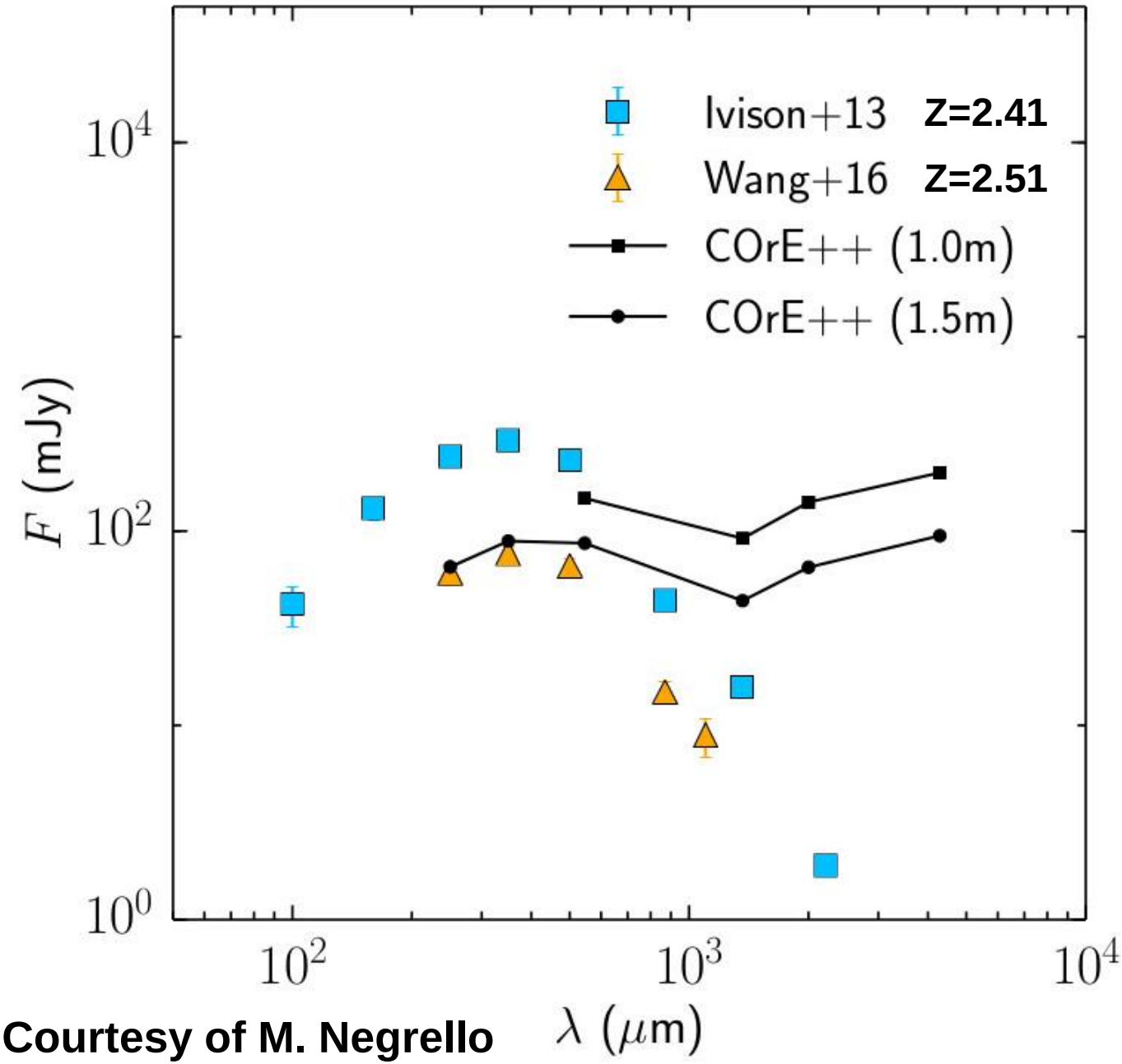

Courtesy of M. Negrello

- Results of a systematic search for candidate high-z objects on *Planck* sub-mm maps was reported by *Planck* Collaboration XXXIX (2016) who produced a catalog of 2151 “cold” sub-mm sources, detected in the cleanest 26% of the sky, with flux density at 545 GHz above 500 mJy. This is referred to as the *Planck* high-z, or PHz, sample.
- The spectral energy distributions, peaking between 353 and 857 GHz at a 5' resolution, are consistent with z> 2.
- *Planck* Collaboration XXVII (2015) accrued follow-up observations with *Herschel*/SPIRE of 234 “cold” *Planck* sources (3 programmes; PIs: H. Dole and L. Montier). Usable results were obtained for 228 of them, including 83 of the 203 sources within the area covered by the PHz sample.
- About 94% of the *Planck* objects were found consistent with being galaxy overdensities, and were considered as proto-cluster candidates. Seven sources (about 3%) are strongly gravitationaly lensed galaxies with spectroscopic redshifts in the range z=2.2 – 3.6 (Cañameras et al. 2015), confirming the effectiveness of the selection criterion based on sub-mm colours.

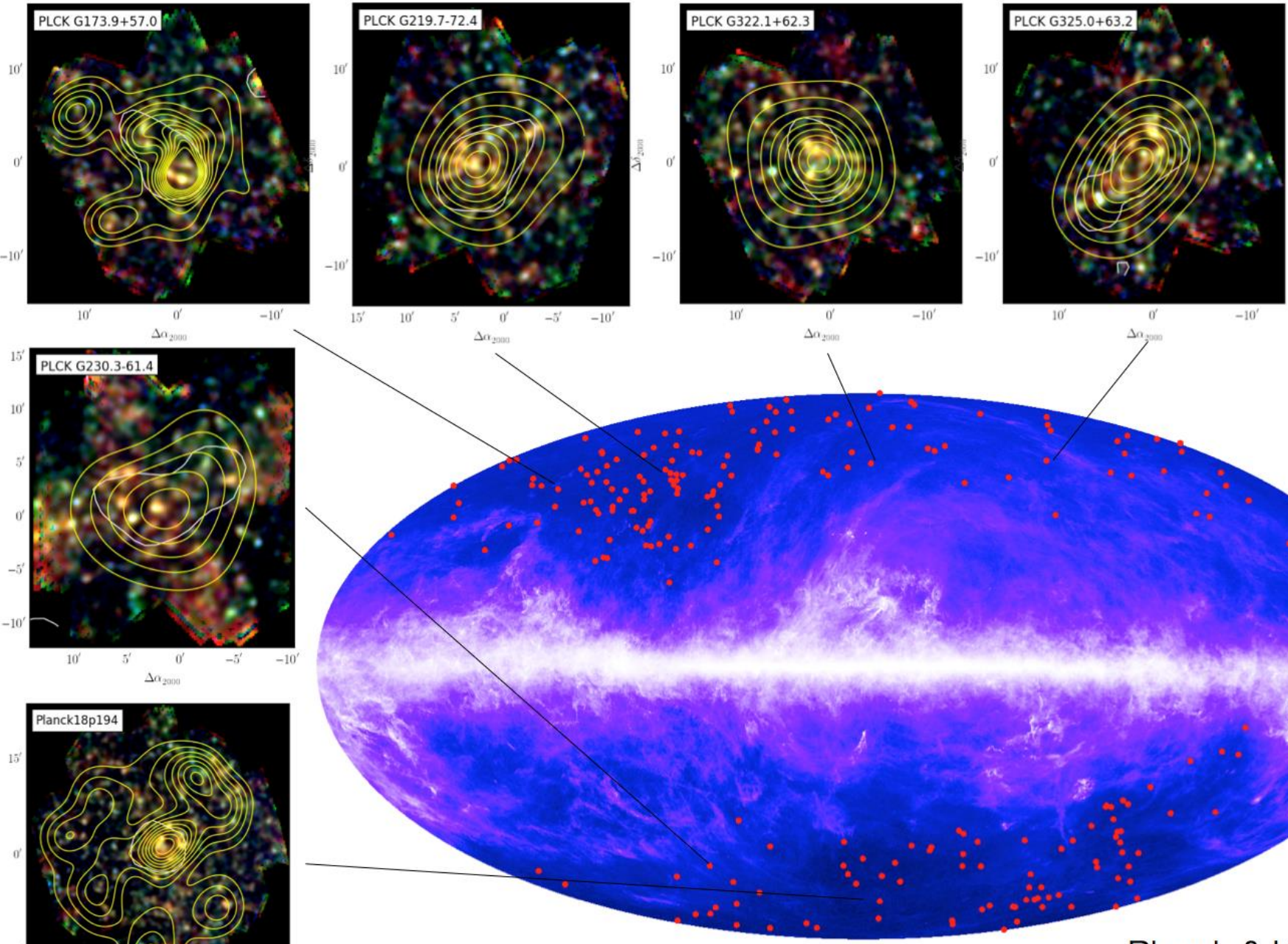

Planck intermediate results. XXVII (2015)

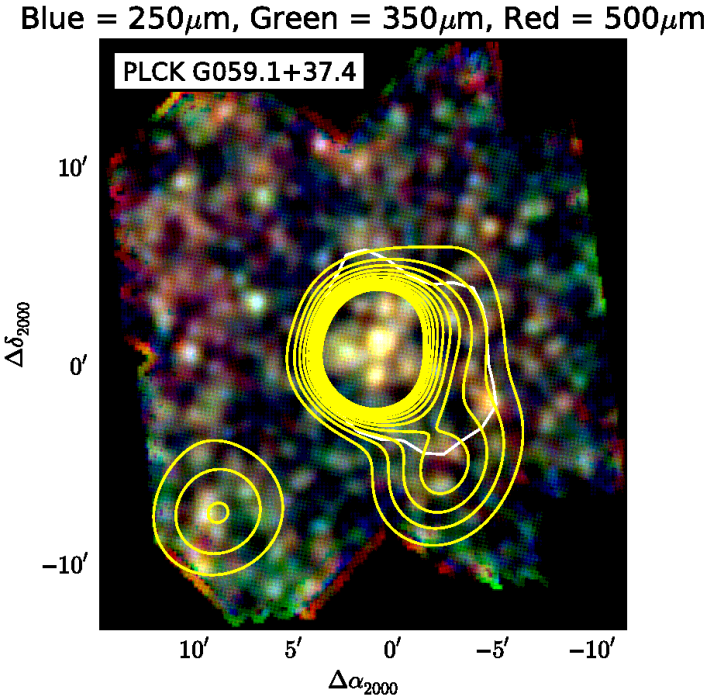

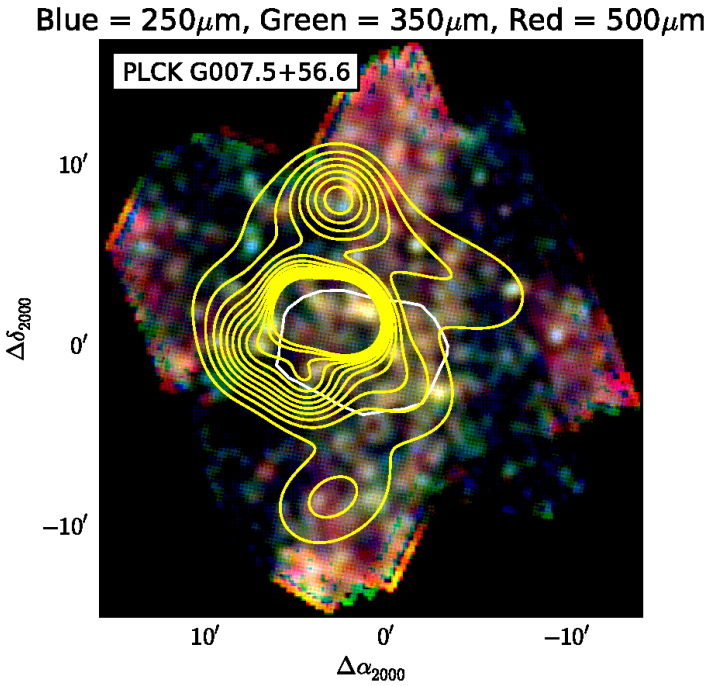

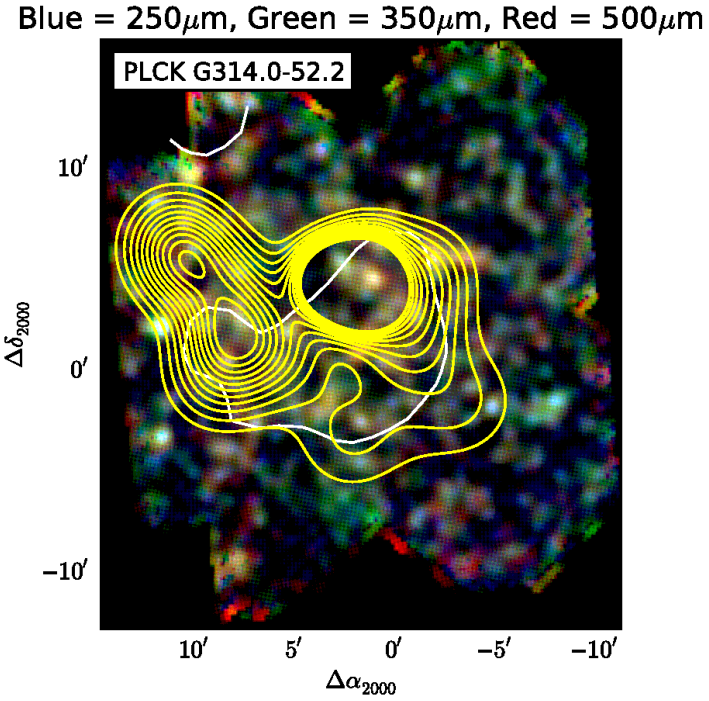

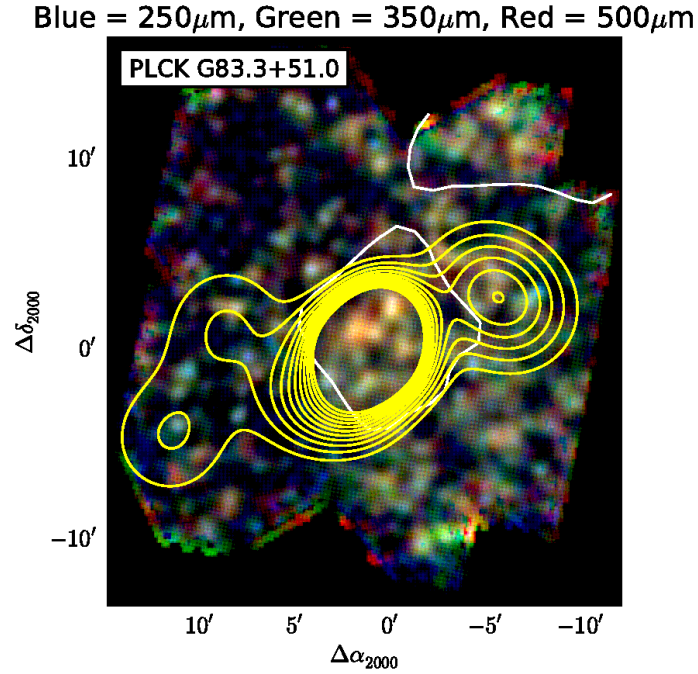

Herschel/SPIRE images of representative *Planck* targets: blue, 250μm; green, 350μm; and red, 500μm. The yellow contours are the significance of the overdensity of 350μm sources, plotted 2σ, 3σ, 4σ, etc.. From *Planck* Collaboration XXVII (2015) .

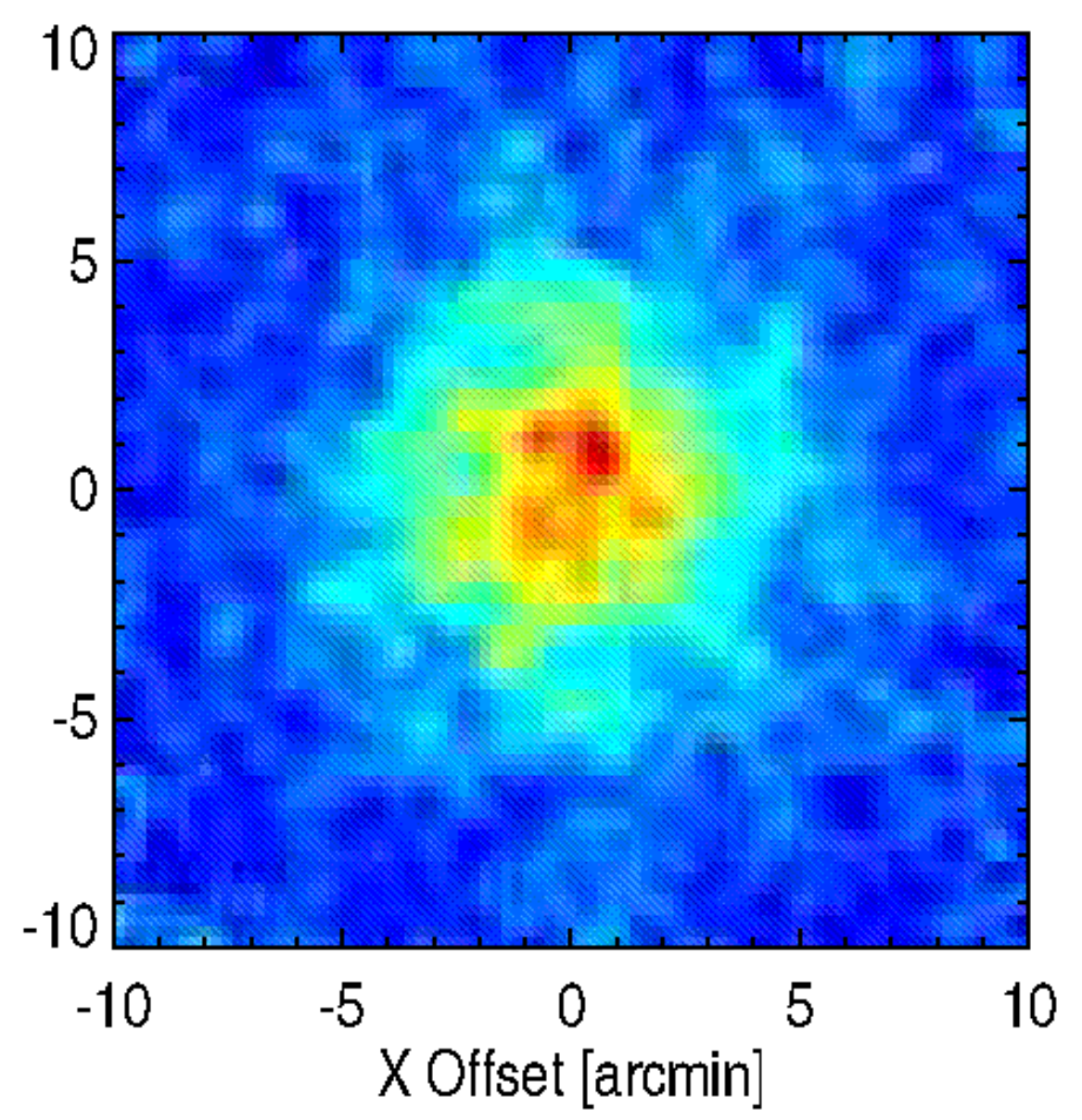

Stacking of the 20′ × 20′ cutouts at 500 μm, over the 83 sources included in the PHz obtained on the 500 μm *Herschel*-SPIRE intensity maps (*Planck* Collaboration XXXIX 2016). This paper recognized that it is impossible to establish whether they are physically bound systems or just random fluctuations. They however argued that “the total number of PHZ source candidates and the expected numbers of massive high-z galaxy clusters are about the same order of magnitude”.

- The distribution of the total (8—1000 μm) IR luminosities of overdensities peaks around 2×10^{14} $L_\odot$ for their reference dust temperature of 35 K. The corresponding SFR is $\approx3\times10^{4}$ $M_\odot$ yr^{-1}.

- The associated halo mass, M_h, can be estimated using the SFR–M_h relation at z=2 derived by Aversa et al. (2015) exploiting the abundance matching technique for a duration of the starburst phase of 0.5–1 Gyr. For mean SFRs in the range 30–1000 $M_\odot$ yr^{-1} the halo masses of star-forming galaxies add up to $M_{h,sf} \approx 5\times10^{14}$ $M_\odot$, independently of the SFR.

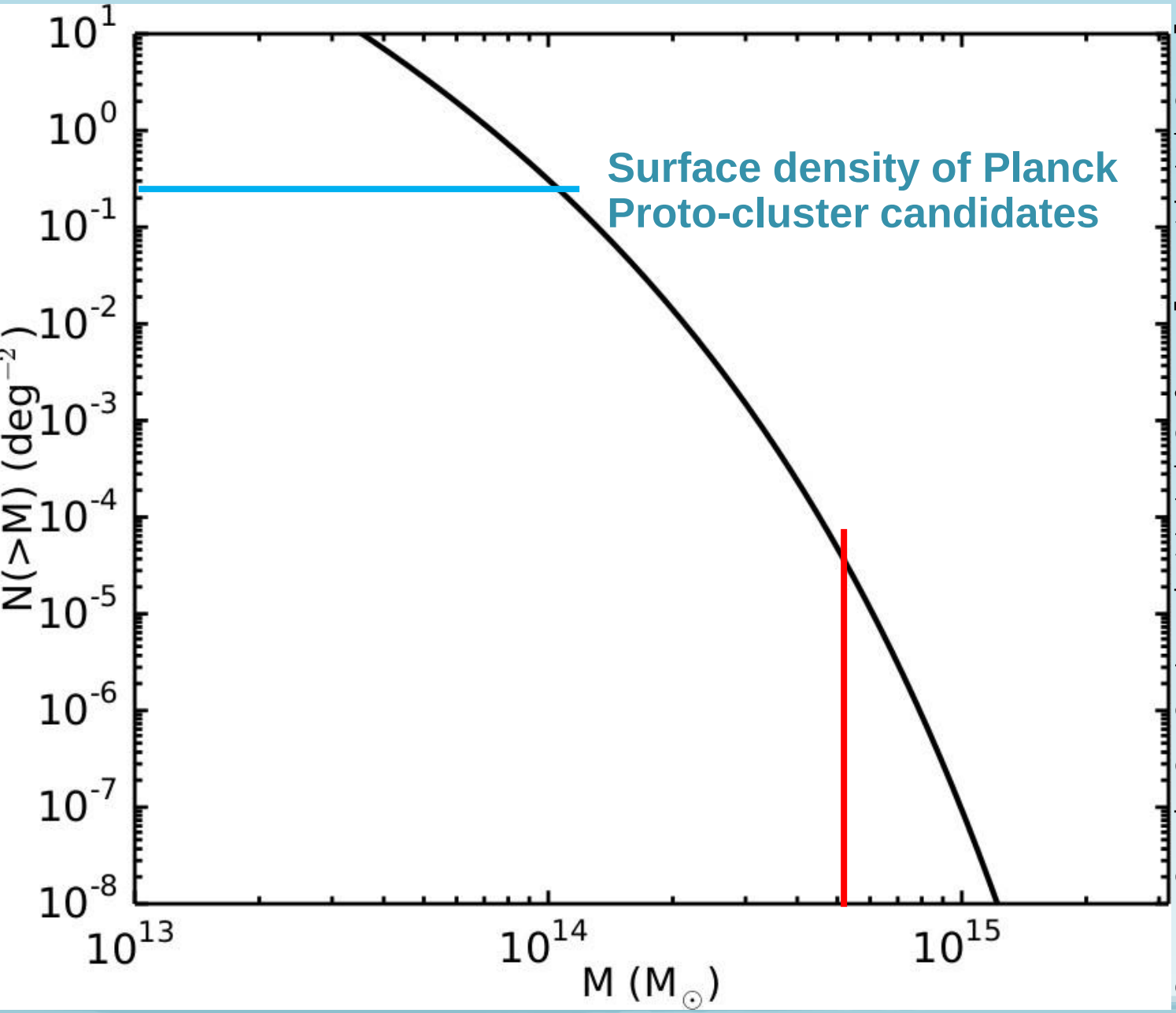

The redshift-dependent halo mass function by Sheth & Tormen (1999) gives a surface density of halos with mass larger than $M_{h,sf}$ at $z \geq 2$ of 5×10^{-5} deg^{-2} to be compared with the surface density of Planck overdensities of 0.21 deg^{-2}.

Higher resolution observations with Spitzer and Herschel showed that the **high-z proto-cluster angular sizes are much smaller than the resolution (5′) used to look for proto-cluster on Planck maps**:

- the study by Alberts et al. (2014) of 274 clusters with $0.3 < z < 1.5$ using Herschel/SPIRE 250 μm imaging, showed that the density of IR-emitting cluster members dominates over the background level only within 0.5 Mpc of the cluster centre. In the z range 1.5–2.5 this scale to an angular scale of about 1′.
- A sub-mm selected proto-cluster core at z=2.41 with an angular size of ≈ 20″ was detected by the Herschel-ATLAS survey over an area of 330 deg² (Ivison et al. (2013).
- A proto-cluster core with similar size and redshift (z≈2.51) was found by Wang et al. (2016).
- Chen et al. (2016, ApJ, 831, 91) have found a strong excess at $\theta \leq$ 10″–20″ in the angular correlation function of sub-millimeter galaxies with redshifts z ~ 1–5 over extrapolations from larger scales.

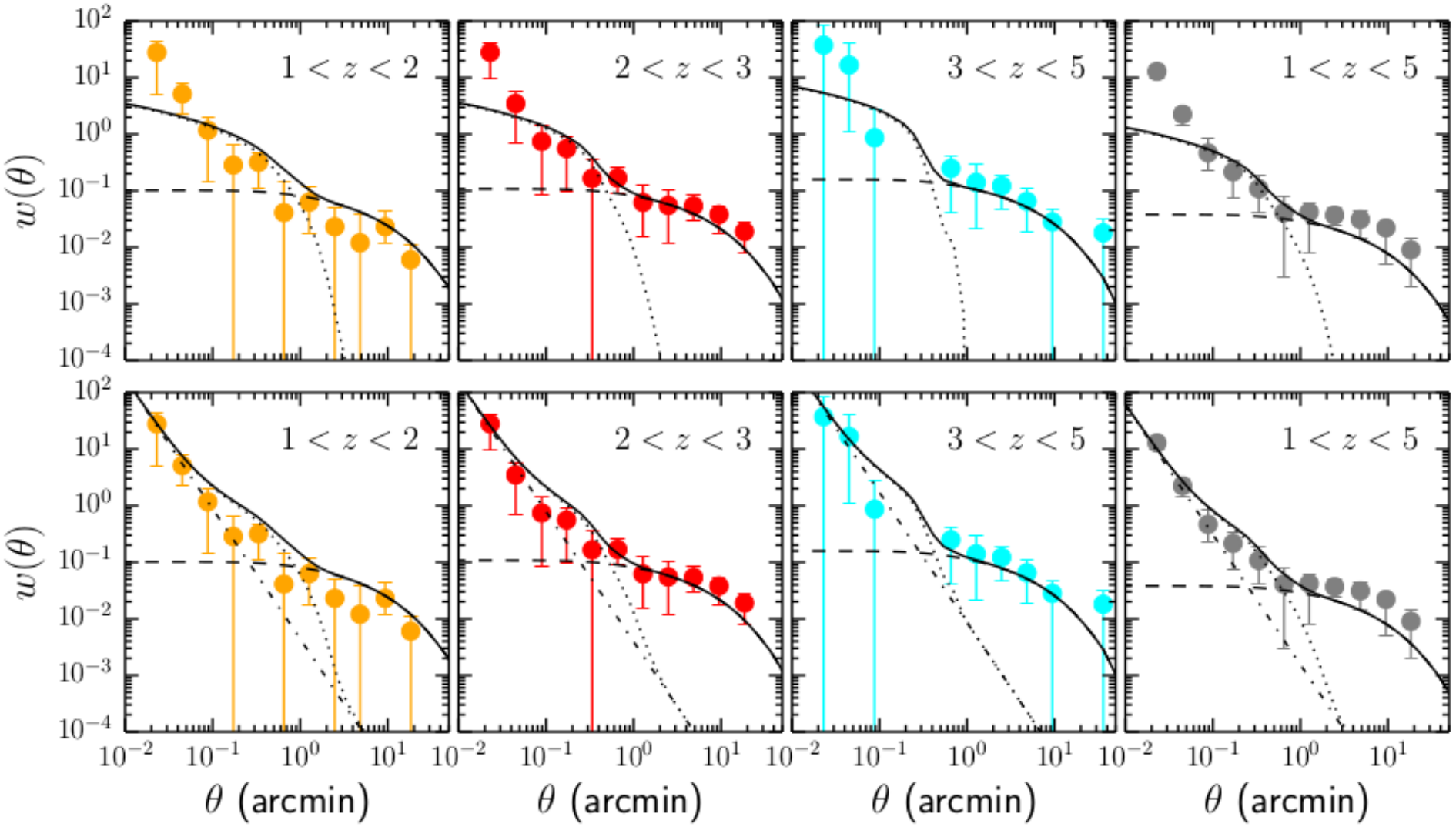

Angular correlation function of sub-mm galaxies in the range z=1 – 5 measured by Chen et al. (2016). The dotted and dashed lines show the 1-h and 2-h contributions, respectively (Cai et al. 2013); the dot-dashed line is an additional contribution introduced by Negrello et al. (2017) to account for the observed small-scale excess. Figure from Negrello et al. (2017).

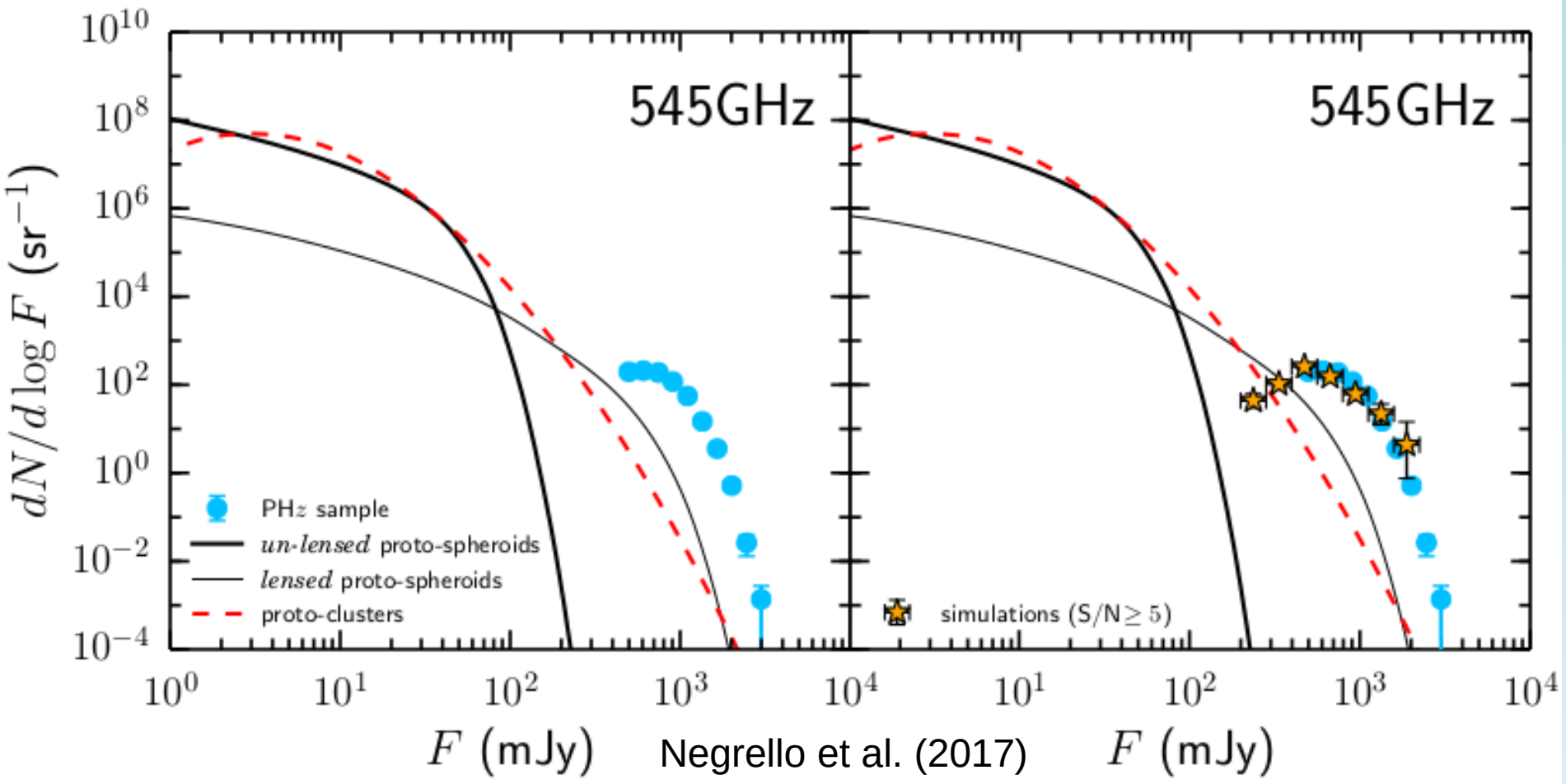

Planck counts of candidate high-z proto-clusters are accurately reproduced by simulations as Poisson fluctuations of the number of unrelated proto-clusters within the *Planck* beam.

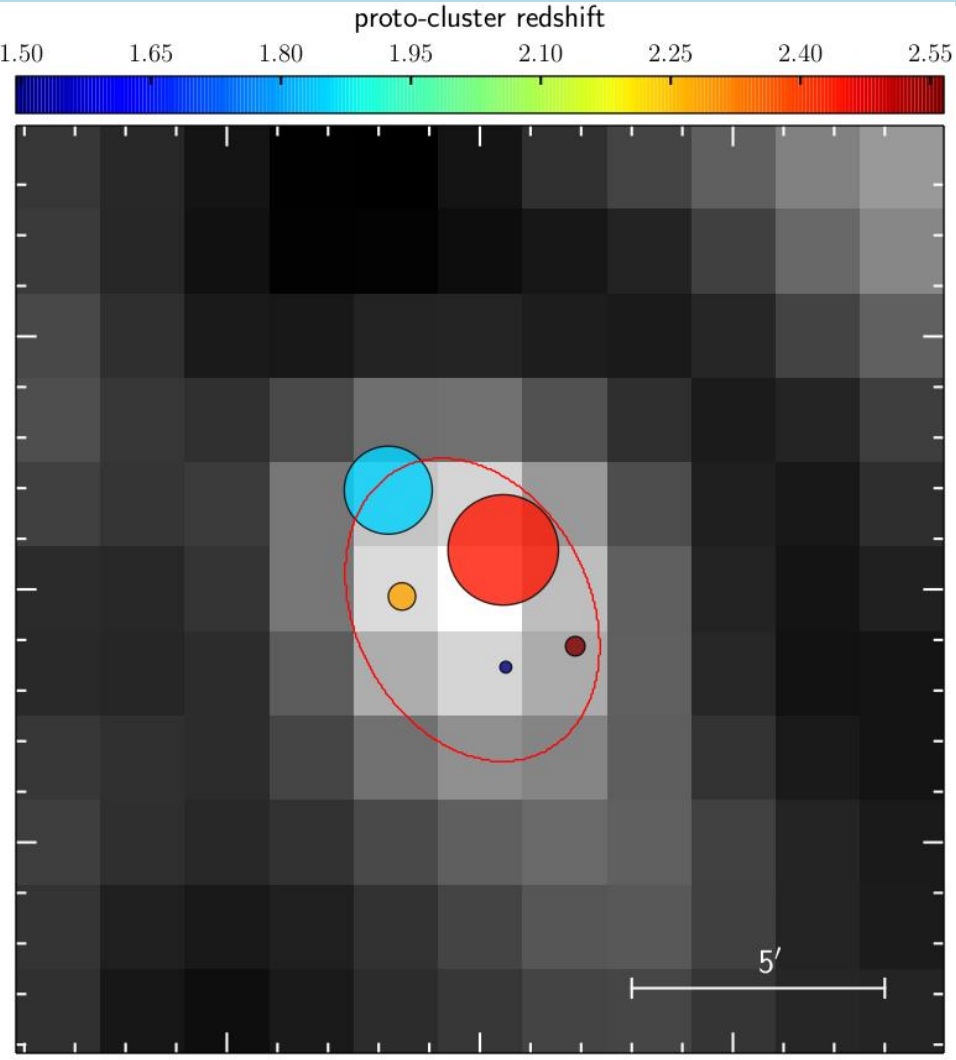

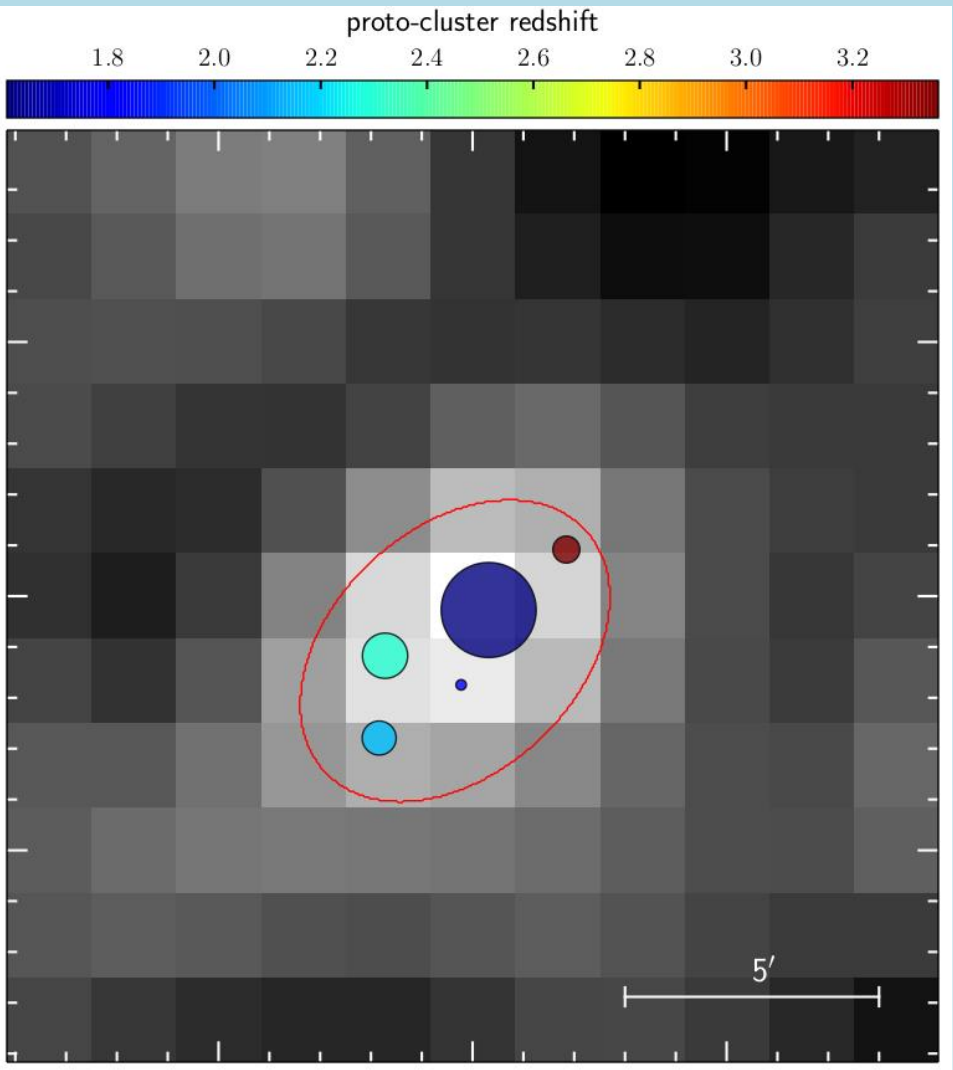

Examples of sources detected in the 545 GHz simulated map. The red ellipsis is the Gaussian fit to the detection, while the spots mark the five brightest proto-clusters within the ellipsis, scaled in size according to their flux density (i.e. the brighter the clump, the bigger the spot). The colours correspond to the redshift (see scale on top of the figures. From Negrello et al. (2017).

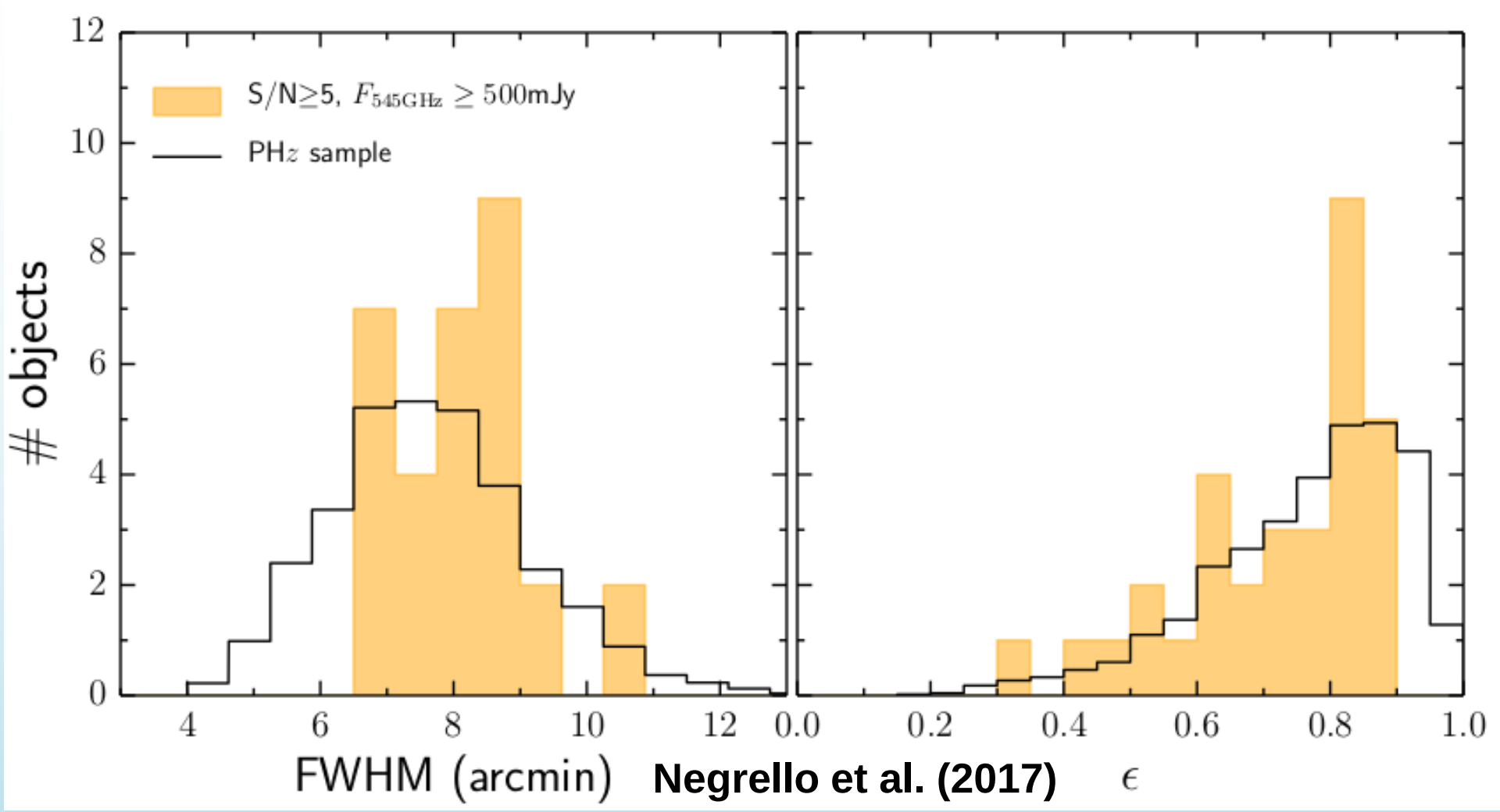

Distributions of FWHMs and of ellipticities of candidate proto-clusters from simulations compared with observational estimates by *Planck* Collaboration XXXIX (2016). Note that simulations cannot reproduce in detail the complex proto-cluster selection procedure by the *Planck* Collaboration.

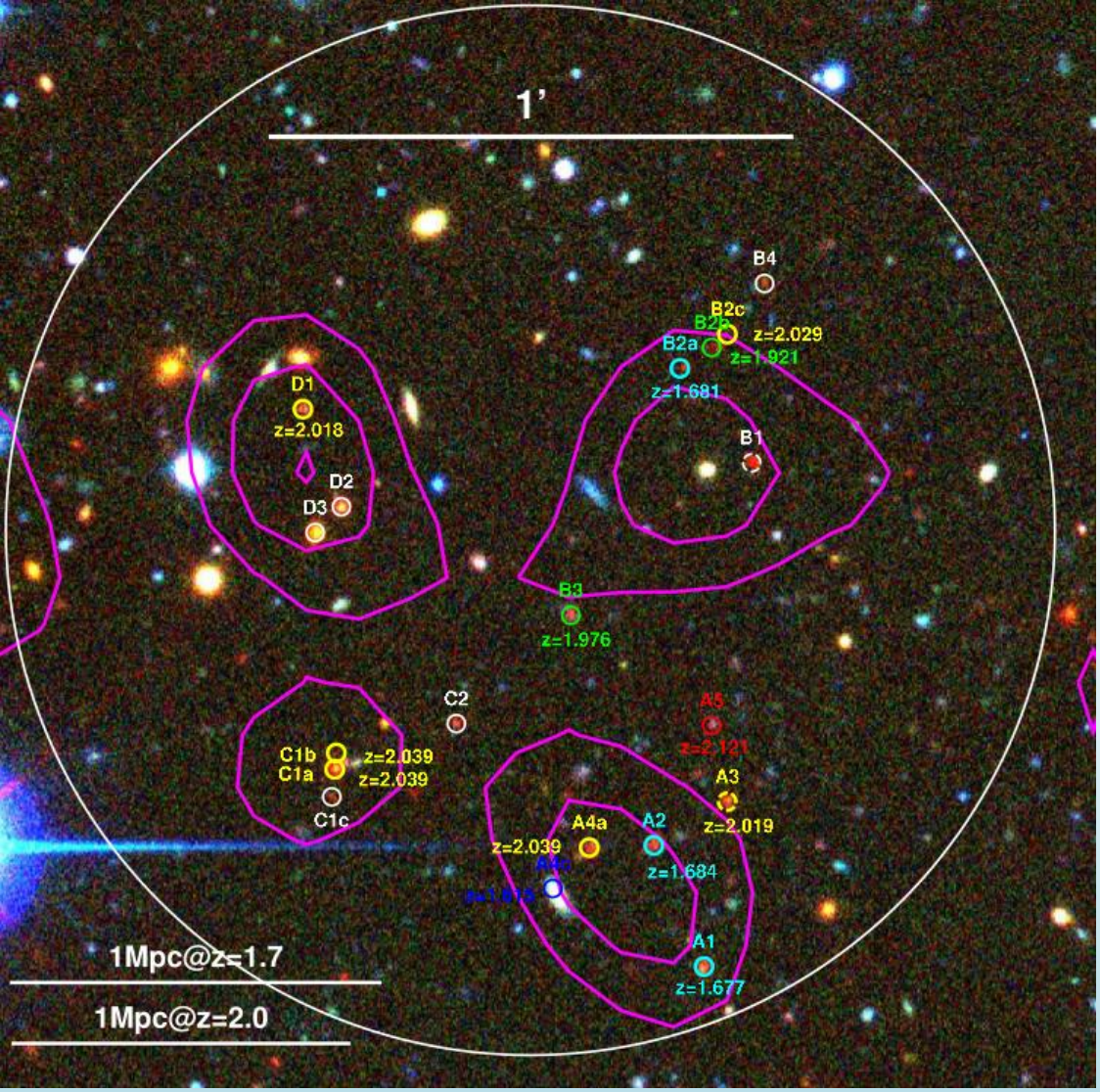

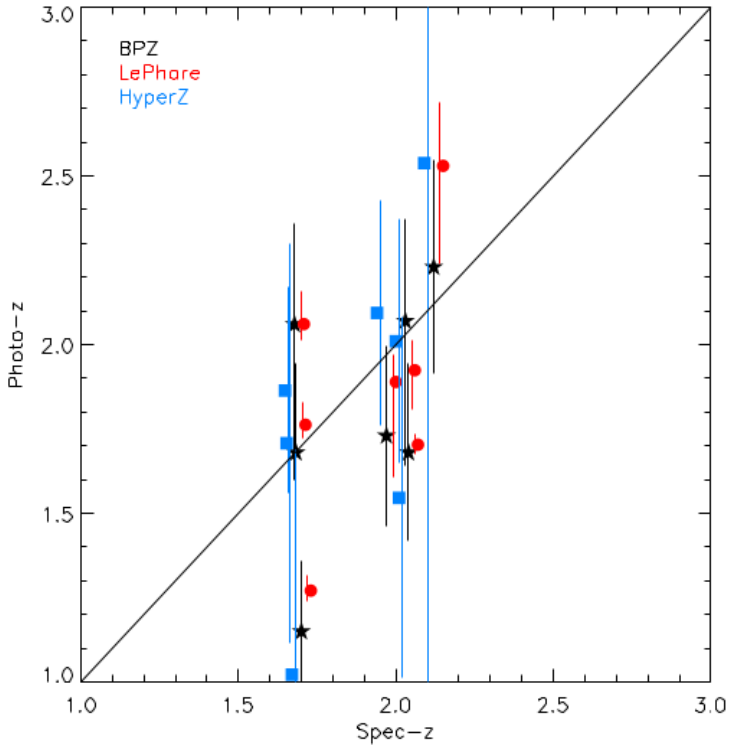

The Planck high-z protocluster candidate PHzG95.5 −61.6 is resolved into two structures at z ≈1.7) and yellow (z ≈ 2.0).

Ks image centered on the position of the high-z proto-cluster candidate PHzG95.5−61.6. The contours of the 250 μm Herschel/SPIRE map are over-plotted in magenta. These galaxies have been colour-coded according to their spectroscopic redshifts from dark blue (closest galaxy, i.e. A4c, z = 1.615) to red (furthest, A5, z = 2.121). For reference, a circle of 1′ radius is shown in white.

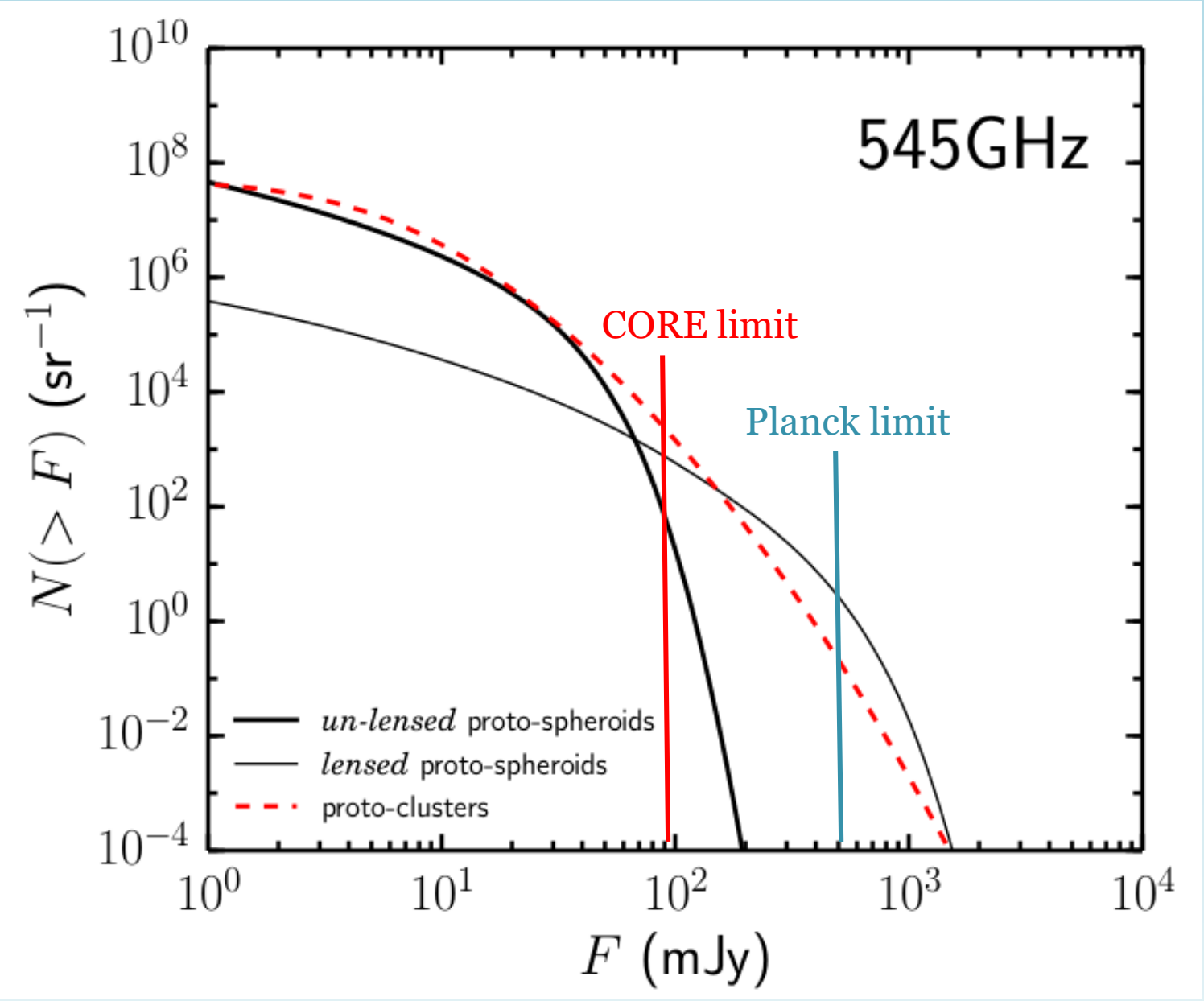

Integral counts of model proto-clusters compared with unlensed and strongly lensed proto-spheroidal galaxies. CORE can improve by orders of magnitude over Planck. From Negrello et al. (2017).

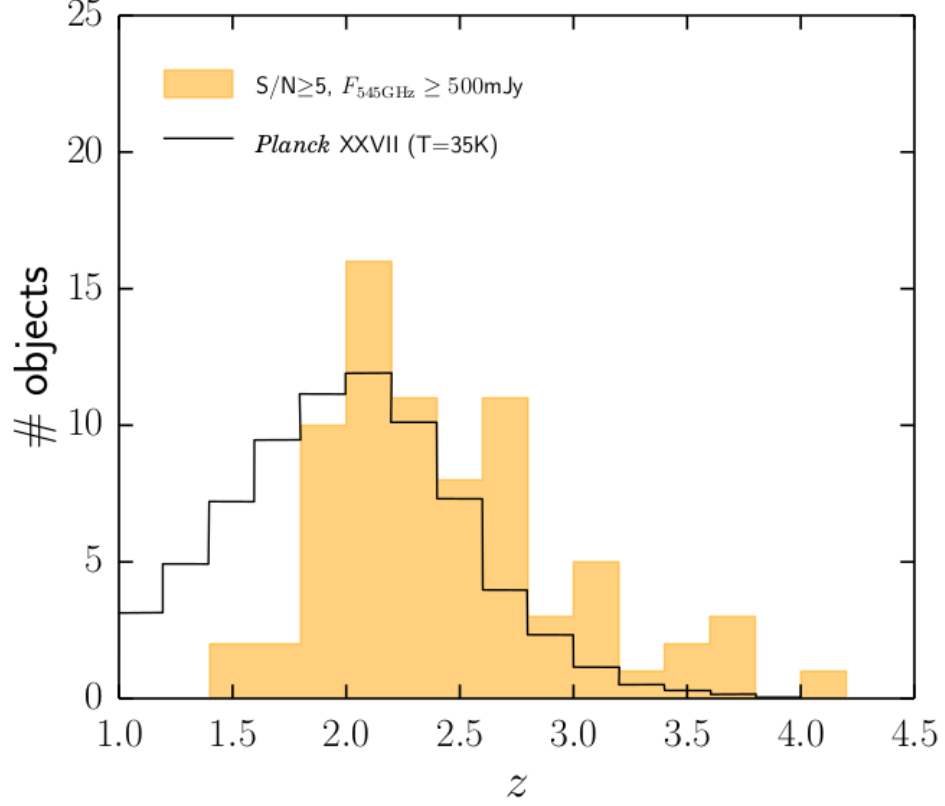

Redshift distribution of the brightest proto-cluster within the Planck beam (from simulations), compared with the estimated redshift distribution of Planck proto-cluster candidates. These objects are good signposts for true proto-clusters at z=2-3. From Negrello et al. (2017).

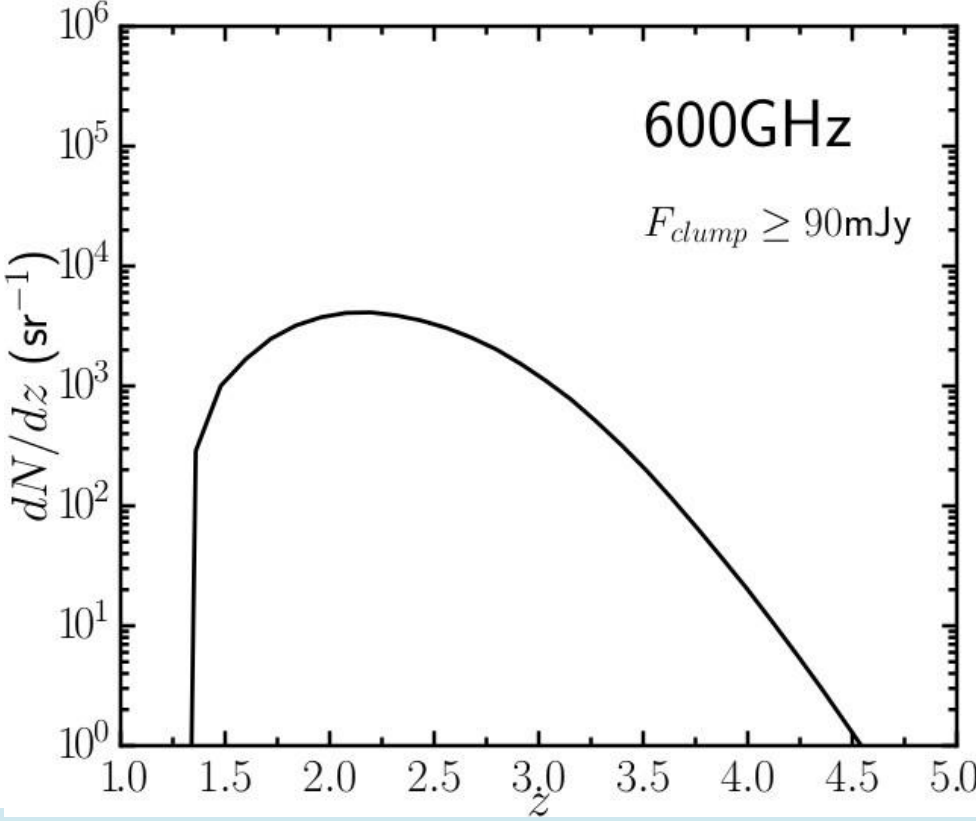

Predicted redshift distribution of proto-clusters detectable by CORE. This instrument could probe the proto-cluster evolution up to z≈4. Courtesy of M. Negrello.

Polarization

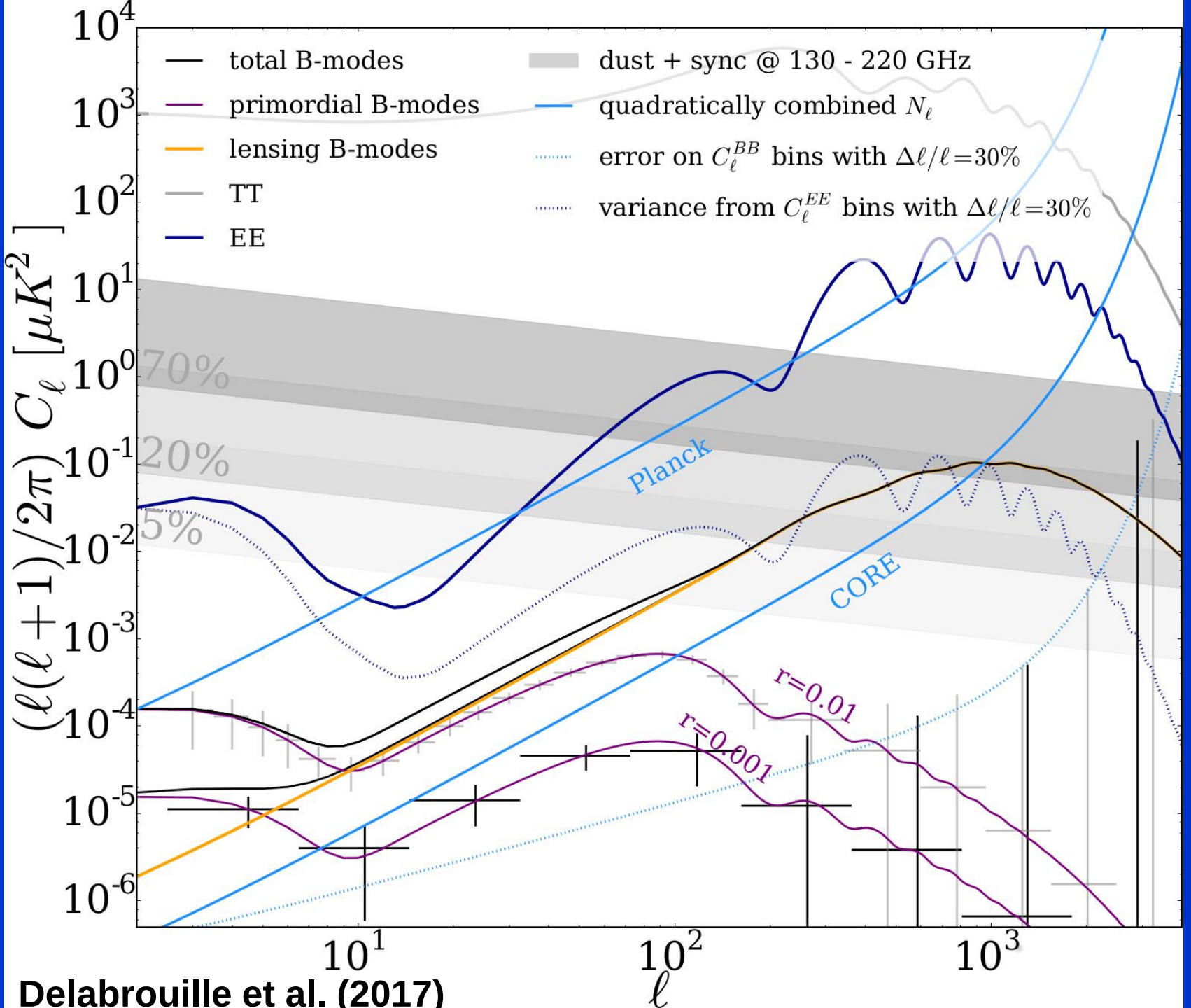

Delabrouille et al. (2017)

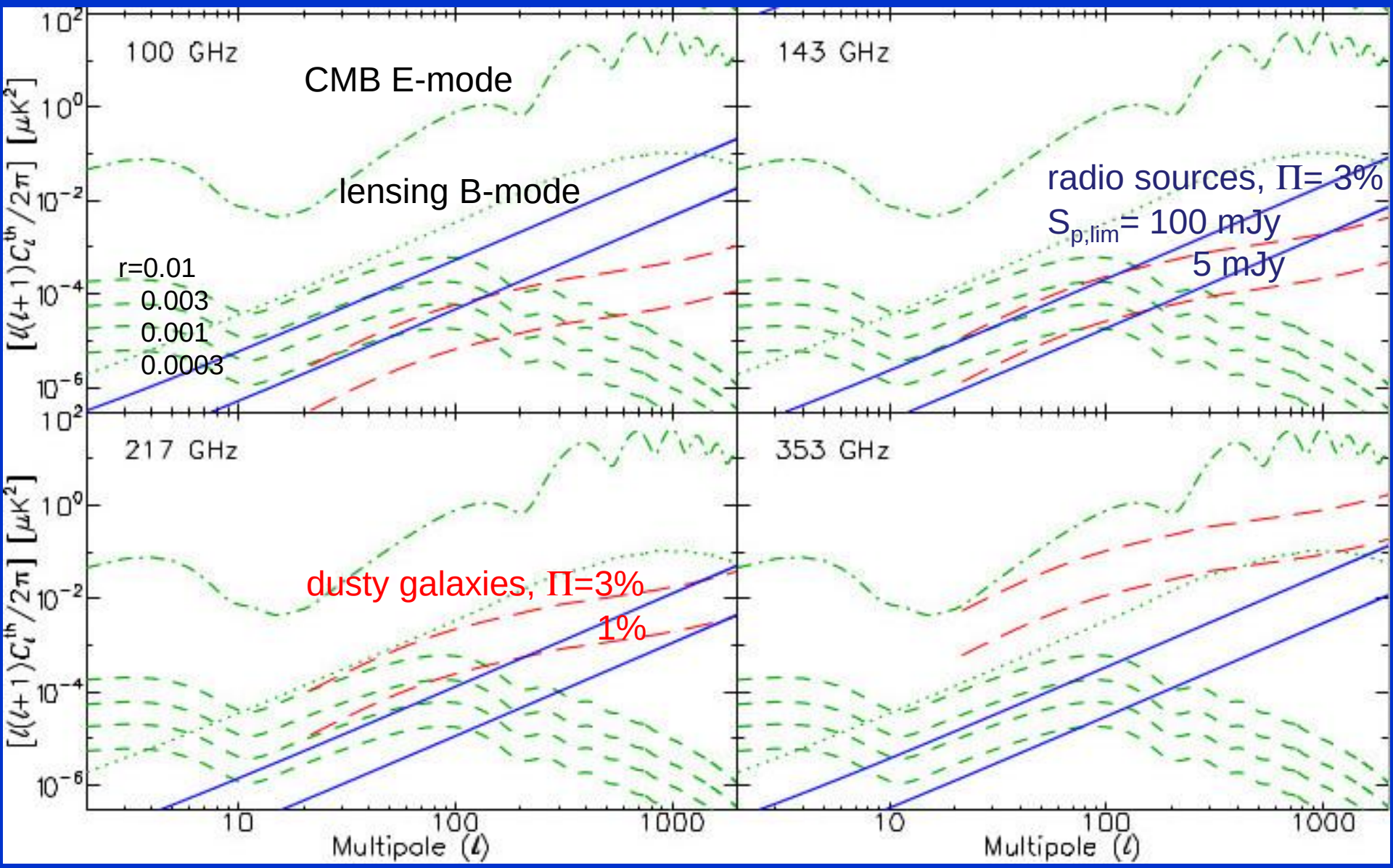

Trombetti et al., in preparation

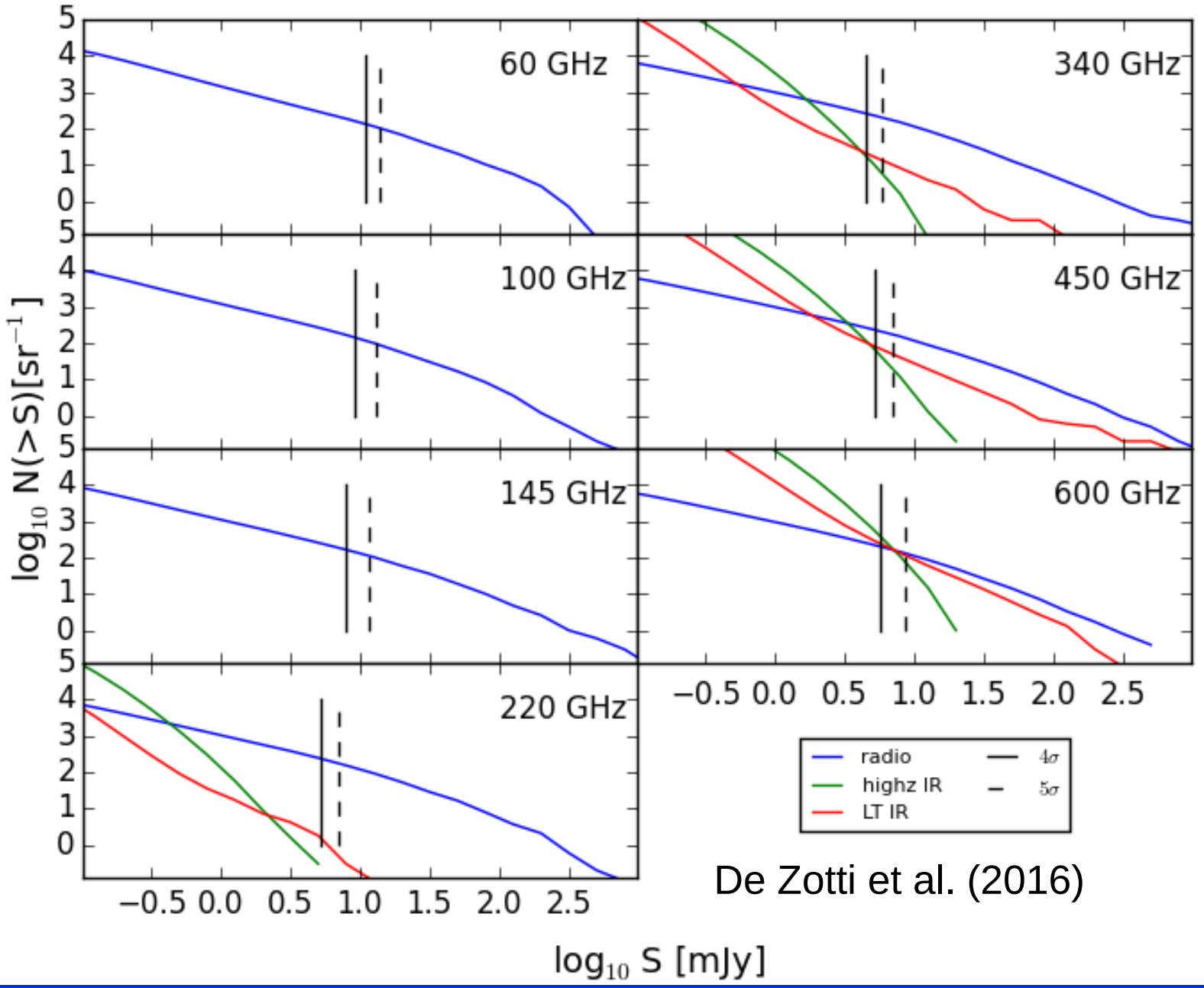

De Zotti et al. (2016)

Predicted counts in polarization for CORE with 1m (dashed) and 1.5 m telescope (solid).

Conclusions - 1

As amply demonstrated by Planck, space-borne CMB experiments thanks to their all-sky coverage and broad frequency range hardly or not accessible from the ground, provide unique information of great astrophysical interest on extragalactic sources.

Examples are:

- **Population properties and SEDs of blazars and of star-forming galaxies**
- **Discovery of extreme strongly lensed galaxies at high-z**
- **Discovery of candidate proto-clusters of galaxies, caught in the pre-virialization phase, when their member galaxies were forming most of their stars**

Conclusions - 2

The substantially better angular resolution and sensitivity of planned next generation experiment like CORE and PICO, even with the same telescope size as Planck, will boost by large factors the number of detections. Great progress in the field also expected from the ground-based CMB-S3/S4 project

But next-generation experiments will also make possible entirely new science such as:

- **The direct detection of large proto-cluster samples up to $z \approx 4$**
- **The study of the evolution of the star-formation in virialized groups and cluster of galaxies**
- **The study of the polarization properties of large samples of radio sources and of dusty galaxies at mm and sub-mm wavelengths**